INTERNATIONAL ATOMIC ENERGY AGENCY
UNITED NATIONS EDUCATIONAL, SCIENTIFIC AND CULTURAL ORGANIZATION

INTERNATIONAL CENTRE FOR THEORETICAL PHYSICS
34100 TRIESTE (ITALY) - P.O.B. 586 - MIRAMARE - STRADA COSTIERA 11 - TELEPHONE: 2240-1
CABLE: CENTRATOM - TELEX 460392 - 1

SMR/291 - 31

SPRING COLLEGE IN CONDENSED MATTER
ON
"THE INTERACTION OF ATOMS & MOLECULES WITH SOLID SURFACES"
(25 April - 17 June 1988)

VIBRATION SPECTROSCOPY ON SURFACES

H. IBACH
Institut für Grenzflachenforschung und Vakuumphysik
KFA Jülich
Postfach 1913
D-5170 Jülich
Federal Republic of Germany

Lectures in Trieste

1 Introduction
2 Electron energy loss spectrometers
2.1. General considerations
2.2. Cathodes
2.3 Monochromators
2.4 Lenses
2.5 Performance of last systems
3. Other techniques for surface vibration spectroscopy
3.1 FT - RIARS
3.2 He - beam scattering
3.3 Comparison of various methods
4. Electron - Solid interaction
4.1 Dielectric Theory
4.2 Electron - core scattering
4.3 Resonance scattering
5. Localized vibrations at Surfaces
5.1 Vibrations and chemical bond
5.2 Selection rules and local symmetry
5.3 Shell Core studies
6. Surface phonons
6.1 Phonons vs. localized vibrations
6.2 Determination of a surface free field - Ni(110)
6.3 Adsorbate induced surface stress and reconstruction
7. Epitaxial metal overlayers
7.1 Ag on Cu(100) and Ni(100)
7.2 Fe on Cu(100), a unique new phase transition.

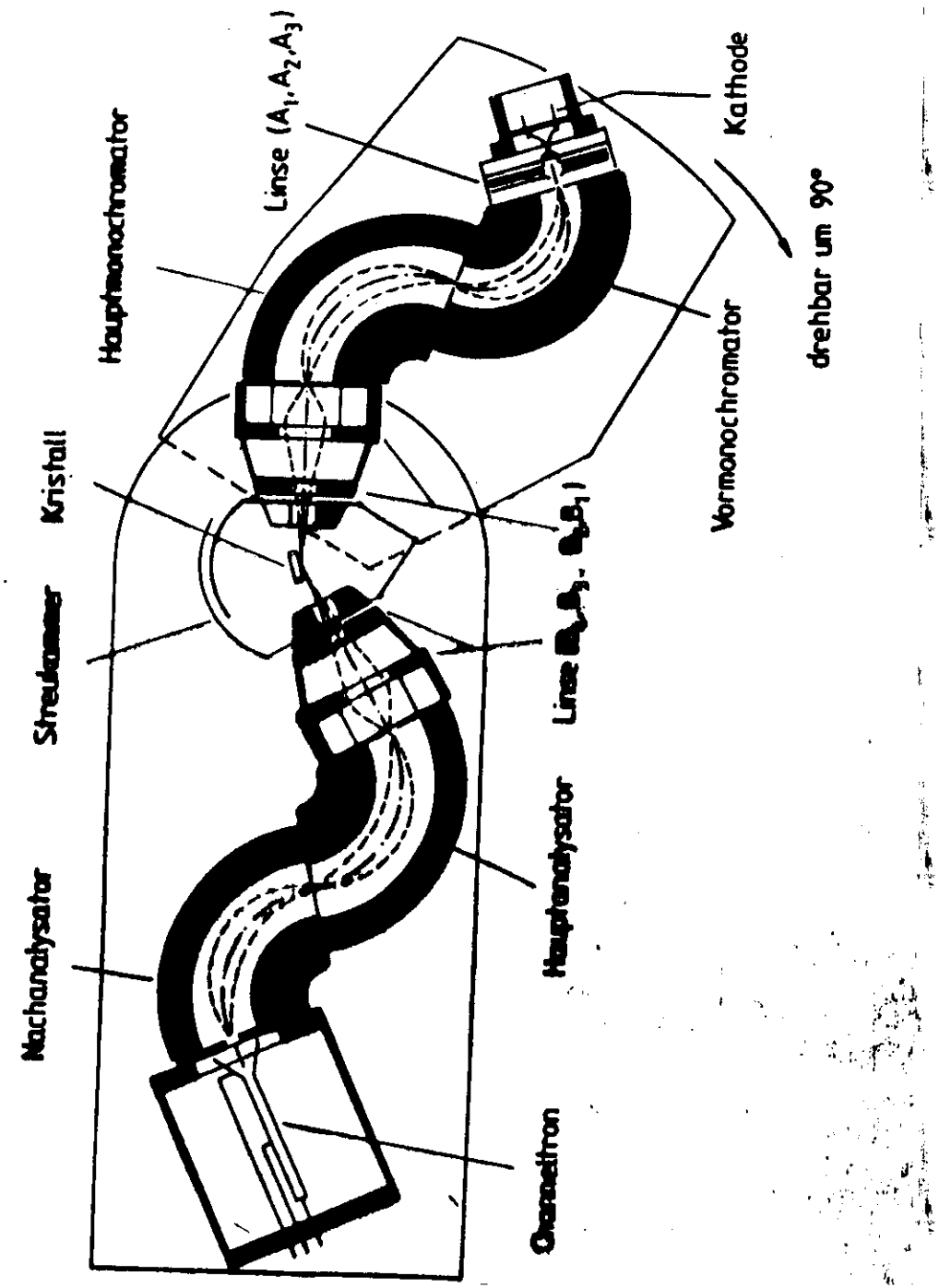

2. Electron spectrometers

2.1 General considerations

Scattering kinematics: Scattering angle
angular resolution momentum space
range of impact energies

Monochromatic current
Optimum resolution

Folie: Current vs. ΔE

$$j_{signal} \sim \Delta E^{-4}$$

2.2 Monochromatic current produced by a cathode

We are interest in the feed current for an electrostatic deflector
If one take a model to the space from the parallel plate arrangement one has to the current

$$I_{feed} = \frac{4}{9} k E_0^{3/2} \frac{hs}{d_k^2} \qquad k = 5.25 \cdot 10^{-6} \, A/eV^{3/2}$$

example $E_0 = 1eV$ $s = 0.3$ $k = 6$ $d_k = 13$

$I = 2.5 \cdot 10^{-8} A$

Energy width of the feed beam $\sim 250 \, mV$

Radiance $= 10^{-10} A / meV$

For 10 meV resolution one has about $10^{-9} A$ at the sample as an upper limit. This is realistic.

How about making d_k shorter?

Folie: Horizontal and vertical Focus of a Kathode - system

Suppose one could further the current passing through the entrance slot, what is the next problem?

2.3 Monochromator with space charge

cylindrical deflector

$$L = m(\dot{r}^2 + r^2\dot{\theta}^2)/2 + c \ln r$$

with $r = r_0(1+\rho)$ and after some algebra one finds the trajectory equation

$$\rho'' + 2\rho + \frac{\Delta E}{E_0} = 2\rho'^2 - 3\rho^2 + \alpha_1^2$$

α_1 entrance angle, E_0 nominal pass energy

first order solution

$$\rho = \frac{1}{\sqrt{2}} \alpha_1 \sin\sqrt{2}\theta + \rho_1 \cos\sqrt{2}\theta + \frac{1}{2}\frac{\Delta E}{E_0}(1 - \cos\sqrt{2}\theta)$$

$$\Rightarrow \quad \theta_f = \frac{\pi}{\sqrt{2}} = 127.28^0$$

$$\rho_2 = -\rho_1 + \frac{\Delta E}{E_0} - \frac{4}{3}\alpha_1^2$$

$$\Delta E_{1/2}/E_0 = \frac{2s}{r_0} + \frac{4}{3}\alpha_1^2$$

Fokic: Trajectories in the ideal cylindrical field

First order effect of space charge is the extension of the focal length. After a long calculation one finds in the limit where the initial focal beam is already monochromatic

$$I_{focal\,max} = 4h\,k\,E_0^{3/2}\,\alpha_{1m}\,\Delta\Theta_f / r_0$$

Fine! only not extending the deflection angle substantially

⇒ Divergence of the beam in the vertical direction

From a model of planar beam we estimate after aquite some calculation

$$\Delta z/h/2 = \pi/4\sqrt{2}\;\Theta_f^2\,\Delta\Theta_f \approx \frac{\pi^3}{8\sqrt{2}}\,\Delta\Theta_f = 2.74\,\Delta\Theta_f$$

$$\text{Transmission } T_2 = \frac{h/2}{h/2 + \Delta z} = \frac{1}{1 + 2.74\,\Delta\Theta_f}$$

Output current:

$$I_{out} = I_{in}\,\frac{\Delta E_{1/2}}{\Delta E_{in}}\cdot T_2$$

$$= \frac{4}{2.74}\,h\,k\,E_0^{3/2}\,\frac{\Delta E_{1/2}}{\Delta E_{in}}\,\alpha_{1m}/r_0$$

$$\alpha_{1m} \sim \sqrt{\frac{3s}{4r_0}}\ (\text{opt.})\qquad \frac{\Delta E_{1/2}}{E_0} = \frac{1}{2}\,\frac{s}{r_0}$$

$$I_{out} = \frac{4}{2.74}\,h\,k\,\frac{\Delta E_{1/2}^{5/2}}{\Delta E_{in}}\,\sqrt{\frac{1s}{4r_0}}\,\left(\frac{2}{3}\right)^{3/2}$$

$$= 0.68\,h\,k\,\frac{\Delta E_{1/2}^{5/2}}{\Delta E_{in}}$$

Example: $h = 6$ $\Delta E_{1/2} = 10\,meV$ $\Delta E_{in} = 200\,meV$

$I_{out} \sim 1\cdot 10^{-9}\,A$

$\Delta E = 5\,meV$

$I_{out} \sim 2\cdot 10^{-10}\,A$

These are realistic numbers. Nevertheless the issue is much more complex and it is extremely difficult to optimize monochromator and cathode with respect to the space charge problem.
Our best design is about a factor of 10 better than this estimate, by invoking a number of tricks, many computer simulations, including space charge and many experimental tests on differently designed spectrometers.

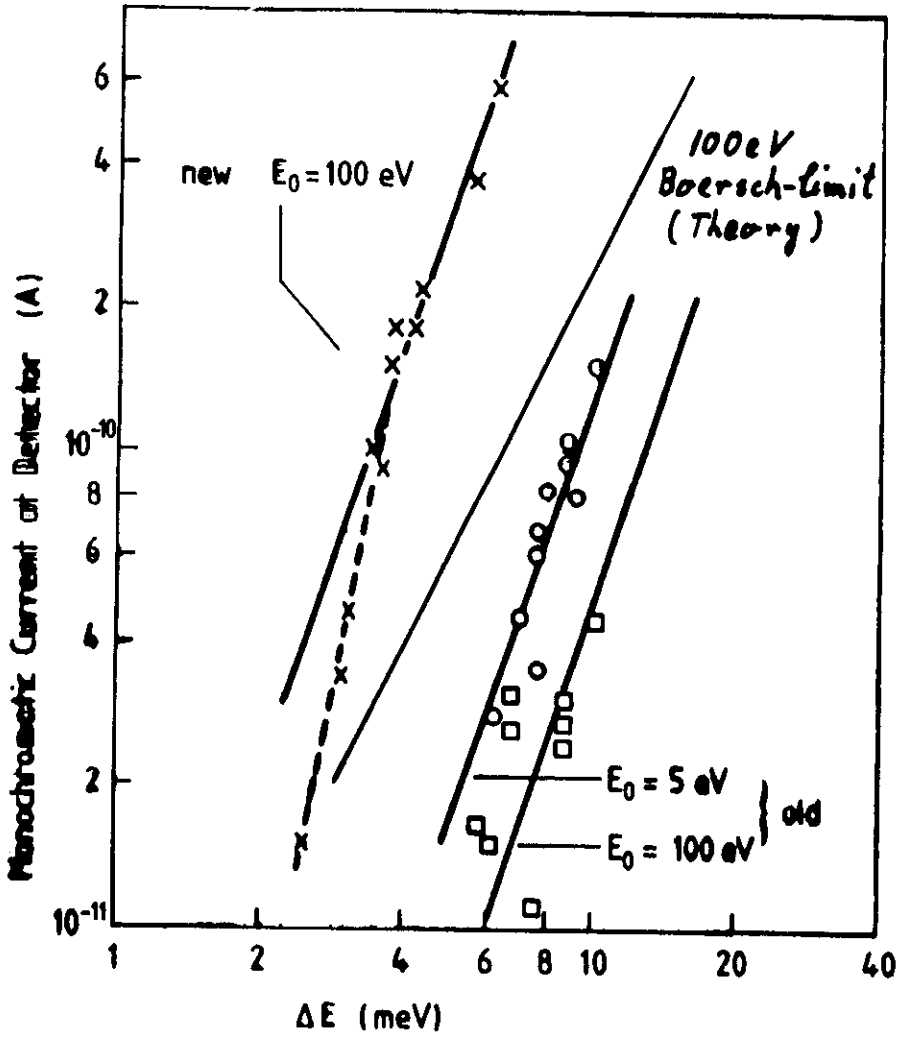

24 Lens systems

Cylindrical Monochromator have exit slits (0.3 × 6 mm). Since one does not need to have a complete deflection for image one optimizes for maximum transmission with minimum number of lens elements. Rectangular lenses are appropriate because of the lack of vertical focussing in cylindrical monochromators. Symmetry of lenses is such C_{2v}.

Abbe's Sine law or phase space conservation then reads

$$\sqrt{E}\, y \sin\alpha = \sqrt{E'} \sin\alpha'\, y'$$

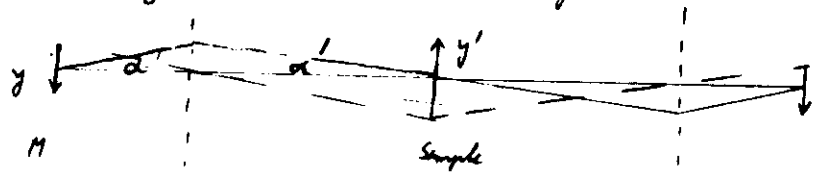

Since the exit angle α of the monochromator is fixed by angular abberations, E by the resolution, α' the angle at the sample is determined by M_y the magnification once E' is chosen. The same holds for the symmetrical lens system between sample and analyzer.
For many applications one wishes a large angle at the sample (large momentum space) simply because of intensity. Large means a small fraction of the Brillouin zone anyway. $\Rightarrow M_y < 1$; lenses close to the sample.
Limitation: angular abberations
space near the sample

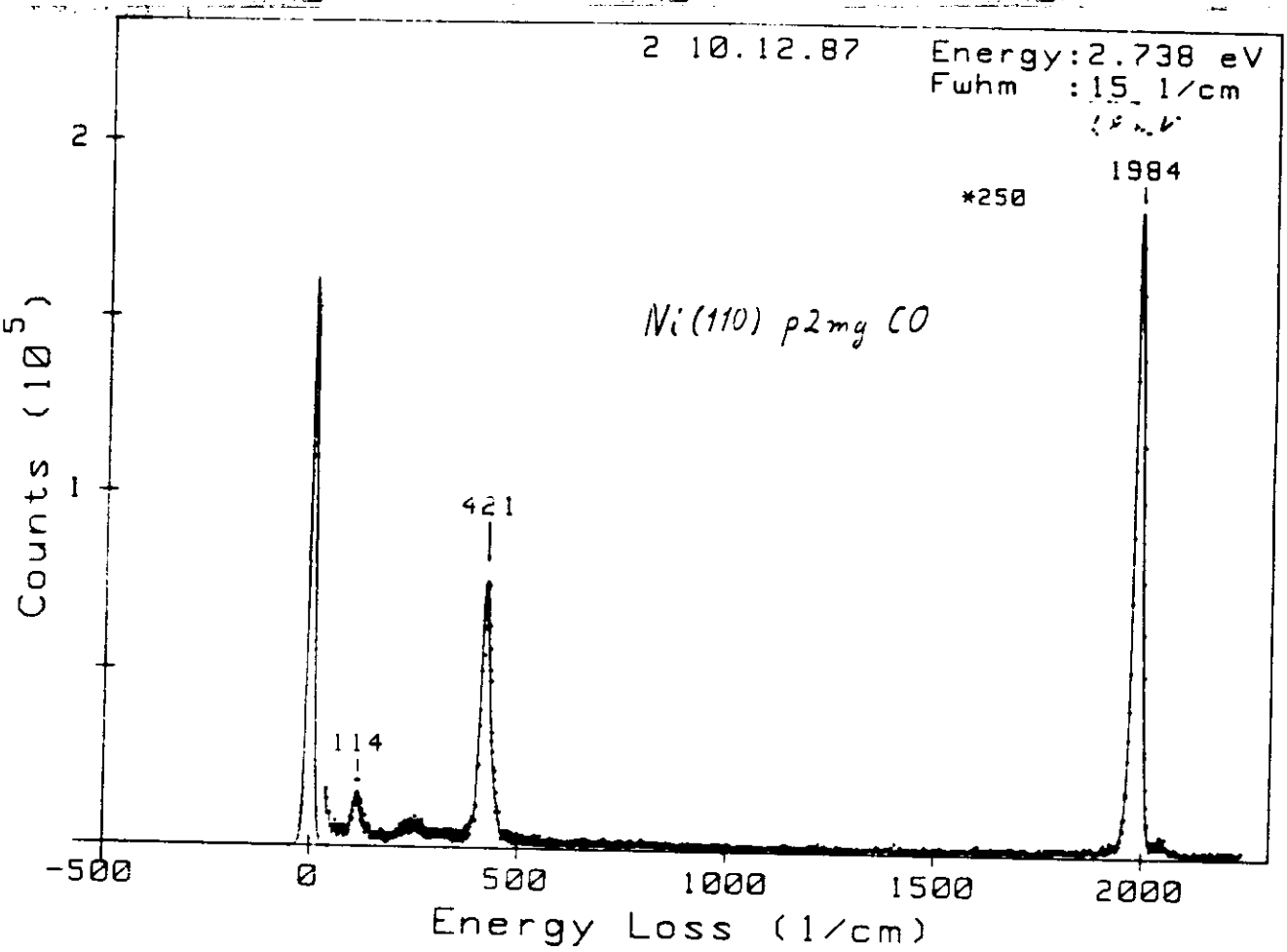
2 10.12.87
Energy:2.738 eV
Fwhm :15 1/cm
1984
*250
Ni(110) p2mg CO
421
114
Counts (10^5)
Energy Loss (1/cm)

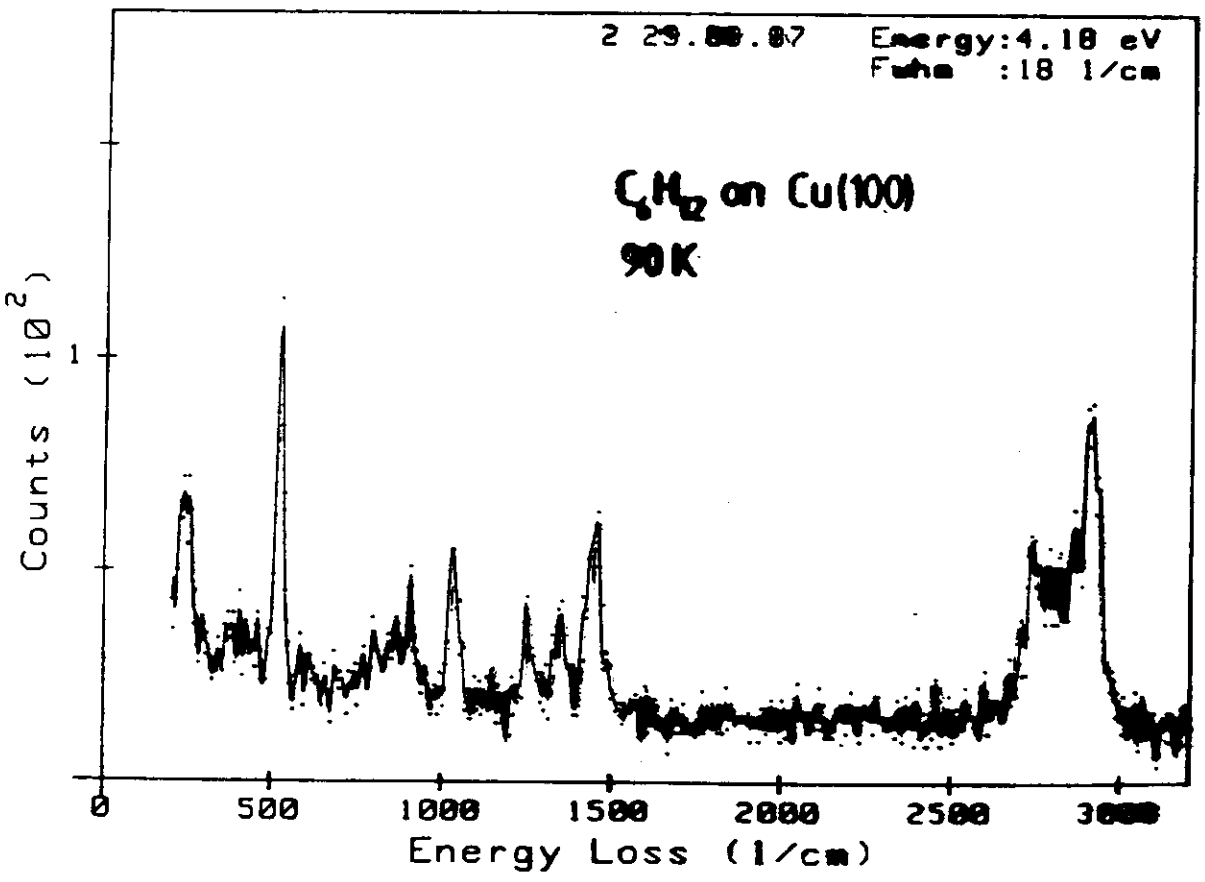
2 29.08.87
Energy:4.18 eV
Fwhm :18 1/cm
C6H12 on Cu(100)
90K
Counts (10^2)
Energy Loss (1/cm)

2.5 Performance of the system
A few examples

Folie: CO on Ni(110)
Hydrocarbon C_6H_{12} on Cu

3.) Other techniques for Surface Vibration spectroscopy
3.1 FT- RIARS
Folie: FT-IR - spectrometer
" : Principle of Fourier-Transform Spectroscopy

Michelson Interferometer

$$\mathcal{E}_1 = \sqrt{I_0/2R(\omega)}\, e^{i\omega t}$$
$$\mathcal{E}_2 = \sqrt{I_0/2R(\omega)}\, e^{i(\omega t + 2\omega x/c)}$$

$$dI(\omega,x) = |\mathcal{E}_1 + \mathcal{E}_2|^2 d\omega$$
$$= (I_0 R(\omega) + I R(\omega) \cos 2\omega x/c)\, d\omega$$

The detector integrates over the ω

$$I(x) = \int I_0 R(\omega)\, d\omega + I_0 \int R(\omega) \cos(2\omega x/c)\, d\omega$$

One measures the change in reflectivity very accurately.
Base line experiment with clean surface
" $R(\omega)$ with adsorbate
Ratio between the two FT-spectra

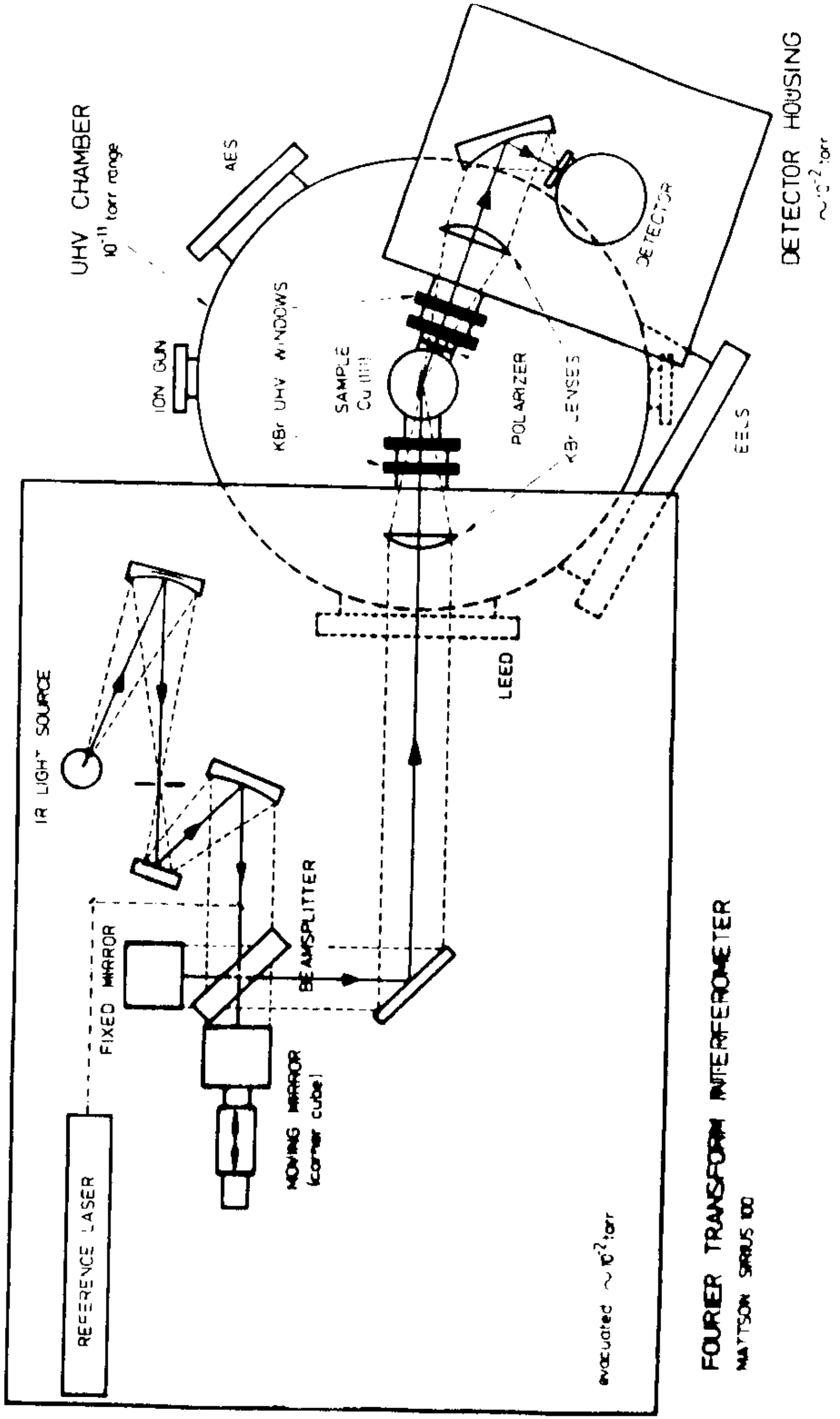

Dr. W. Erley

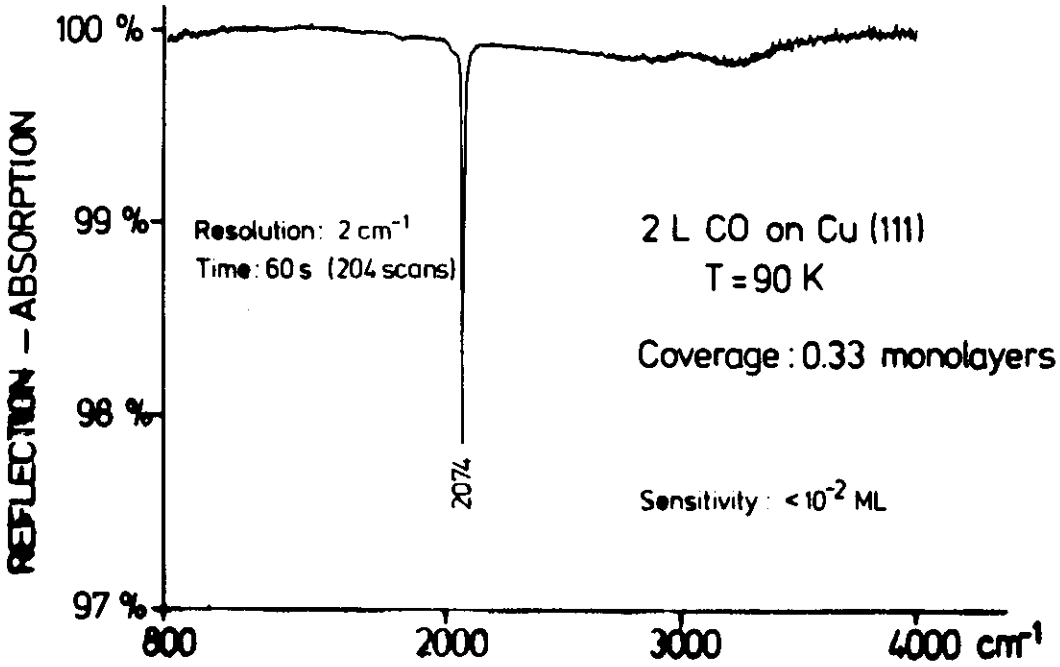
100 %
99 %
98 %
97 %
REFLECTION – ABSORPTION
Resolution: 2 cm⁻¹
Time: 60 s (204 scans)
2074
2 L CO on Cu (111)
T = 90 K
Coverage: 0.33 monolayers
Sensitivity: < 10⁻² ML
800
2000
3000
4000 cm⁻¹

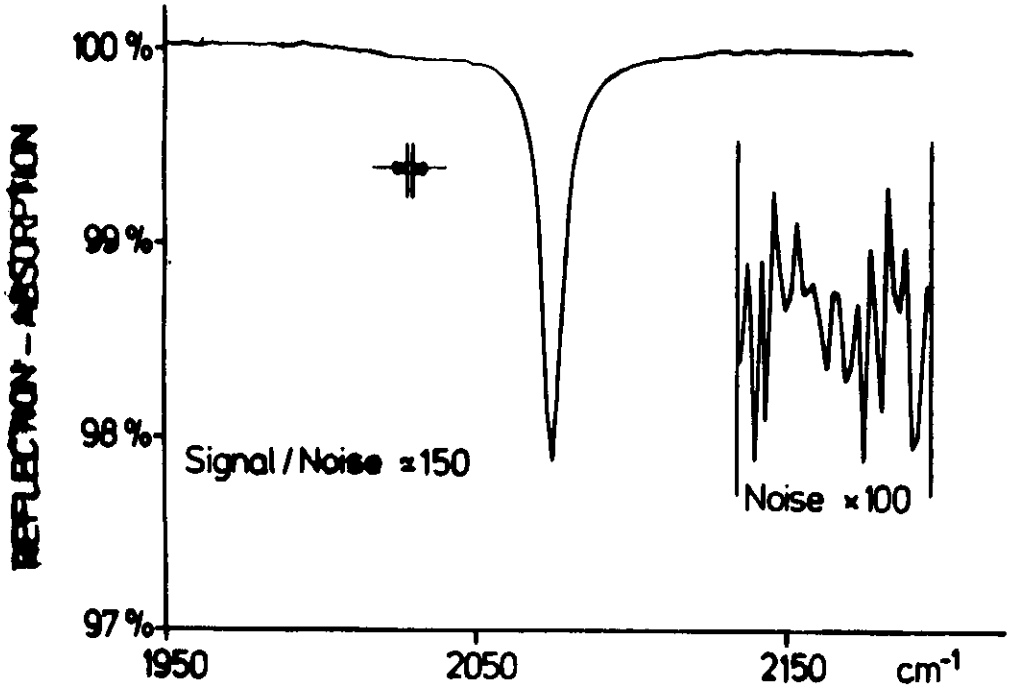
100 %
99 %
98 %
97 %
REFLECTION – ABSORPTION
Signal / Noise ≈150
Noise ×100
1950
2050
2150
cm⁻¹

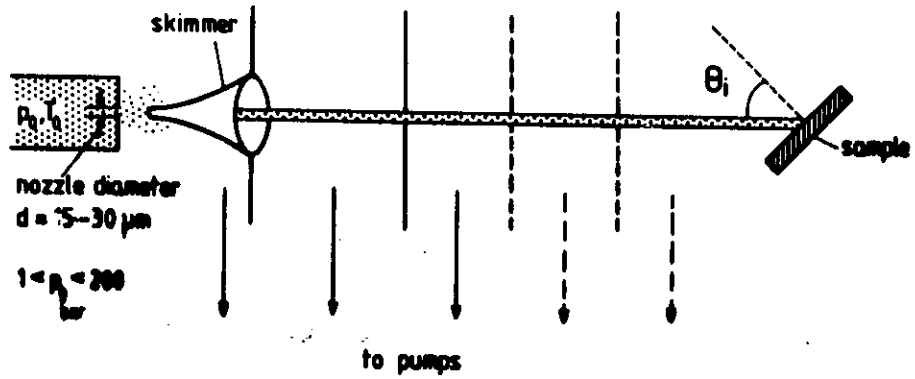
skimmer
θi
sample
nozzle diameter
d = 5–30 μm
to pumps

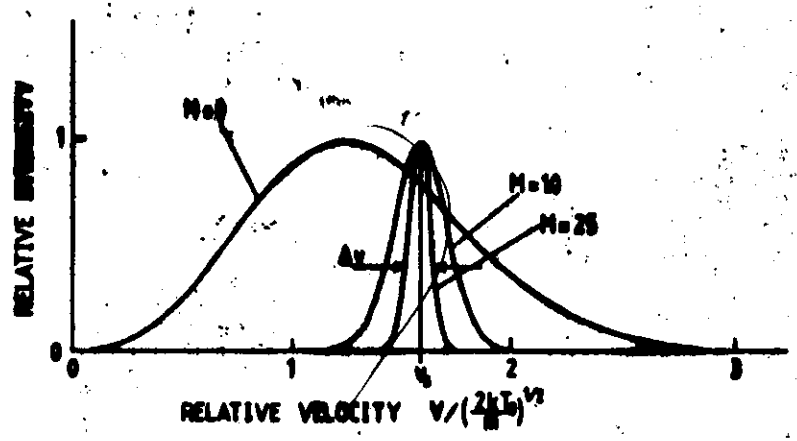
RELATIVE INTENSITY
M=0
M=10
M=20
Δv
1
0
1
2
3
RELATIVE VELOCITY

Inelastic Scattering of He and e⁻

He

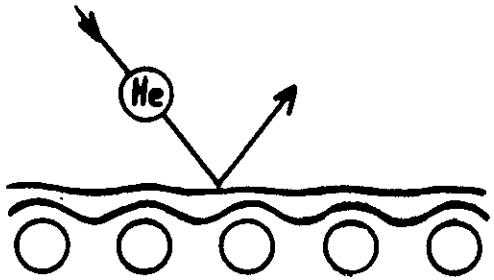

$n \sim 10^{-5}$

e⁻

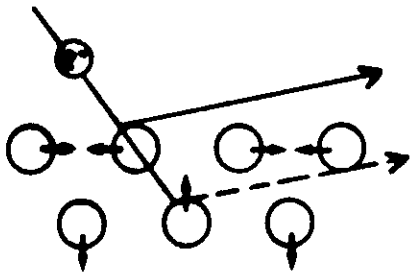

Theory of atom scattering, semi-classical approach

$$\frac{d\sigma}{d\hbar\omega d\Omega} = \left(\frac{m}{2\pi\hbar^2}\right)^2 \frac{k'}{k} |\langle \varepsilon | e^{i\eta(r,t)} | \alpha \rangle|^2 \delta(E' - E - \hbar\omega)$$

$\eta = \frac{1}{\hbar}\int L\,dt$ $\quad L = T - V$ Lagrange Function along the atom trajectory

$L = L_0 + \sum_n \frac{\partial L}{\partial R_n}\Big|_{u_n = 0} u_n$ expansion in term of the lattice coordinates $R_n = R_{n0} + u_n$

$L = L_0 - \sum_n F_n u_n$

$$\eta_{ph}(r_{\parallel}, t) = -\frac{1}{\hbar}\int F_n(r_{\parallel}, t')\, u_n(t + t')\, dt'$$

$r_{\parallel}, t$ time and coordinate of the point of inflection

Even without calculation one sees the following: suppose the atom is slow such that

$$v/\Lambda \ll \omega$$

with ω the phonon frequency and Λ a length parameter of the scattering potential, then the integral vanishes. Quantitatively one should compare the Fourier transform of $F_n(r_{\parallel}, t)$ with the phonon frequency

Ferlin Figure 4 Proc. IX IVC-V ICSS, Madrid (1983)

Note: He - interaction is with the outermost charge contours of the surface atoms

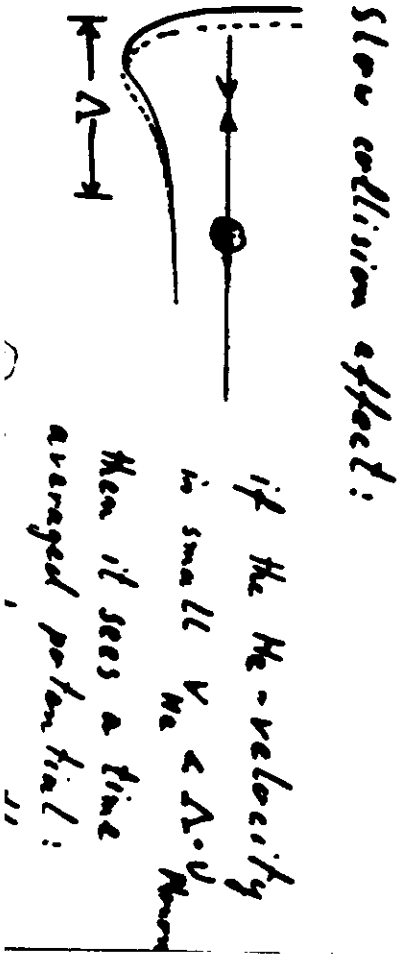

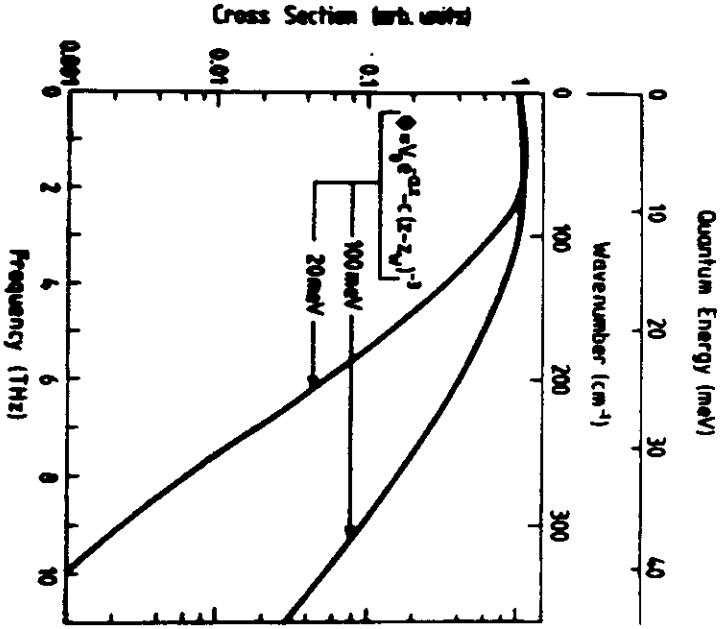

Experimental Methods for Vibration Spectroscopy

	sensitivity in monolayers	surface area	spectral regime	resolution	
IR-transmission	many	m^2	> 1000 cm^{-1}	5 cm^{-1}	finely dispersed material
neutron scattering	many	m^2	< 1000 cm^{-1}	variable	
enhanced Raman	variable	$10^{-2} cm^2$	> 100 cm^{-1}	5 cm^{-1}	special systems and surface conditions
tunnel spectroscopy	10^{-2}	$10^{-2} cm^2$	> 200 cm^{-1}	5-20 cm^{-1}	specially prepared samples
He-scattering	10^{-4} ?	$10^{-1} cm^2$	< 300 cm^{-1}	2 cm^{-1}	phonon-dispersion physisorbed molecules
IR-reflection absorption	$1-10^{-3}$	1 cm^2	> 200 cm^{-1} (limited)	1 cm^{-1}	ambient pressure, limited to the near infrared and dipol active modes
electron energy loss	$10^{-2}-10^{-4}$	$10^{-3} cm^2$	> 40 cm^{-1}	> 15 cm^{-1}	wide spectral range, phonon dispersion, largest versatility

Electron Energy Loss spectroscopy (EELS)

Three scattering mechanisms for low energy electrons

1.) Dielectric or dipole losses

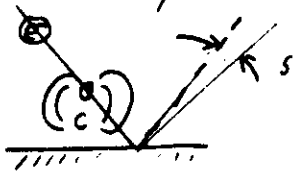

$\sigma \sim E^{-1}$

2.) Scattering from ion cores

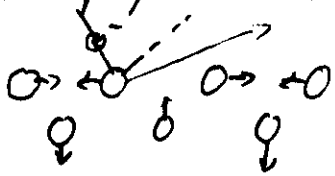

3.) Resonance scattering, shape resonances

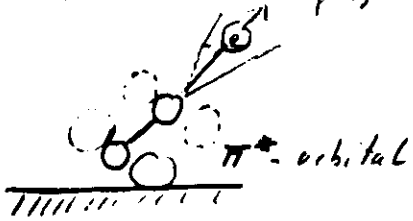

The Theory of Dielectric Energy Losses

We calculate the losses using classical electrodynamics

$$W = \frac{1}{4\pi} \int_{-\infty}^{\infty} dt \int d\underline{r}\ \underline{\mathcal{E}}_i(\underline{r},t) \cdot \underline{\dot{D}}(\underline{r},t)$$

For surface losses a 2D-Fourier expansion:

$$\underline{\mathcal{E}}_i(\underline{r},t) = \int d\omega\, d\underline{q}_{\parallel}\, e^{-i\omega t}\, e^{-i\underline{q}_{\parallel}\cdot\underline{r}_{\parallel}}\, e^{-q_{\parallel}|z|}\, \underline{\mathcal{E}}_i(\underline{q}_{\parallel},\omega)$$

$$\Rightarrow \quad W = 2\pi^2 \int dz\, d\omega\, d\underline{q}_{\parallel}\, \omega\, \varepsilon_2(\omega) \left|\mathcal{E}_i(\omega,\underline{q}_{\parallel},z)\right|^2 e^{-2q_{\parallel}|z|}$$

For a semi-infinite dielectric half space the internal field $\mathcal{E}_i$ is screened by the factor

$$\mathcal{E}_i = \frac{2}{\varepsilon(\omega,q_{\parallel})+1}\ \mathcal{E}_{ext}$$

where $\mathcal{E}_{ext}$ is the external field created by the electron. It follows immediately that the dielectric losses are proportional to

$$P(\omega) \sim \frac{\varepsilon_2}{|\varepsilon+1|^2} = \mathrm{Im}\,\frac{-1}{\varepsilon(\omega,q_{\parallel})+1}$$

When $\varepsilon(\omega)$ is like a free electron gas solid

$$\varepsilon(\omega) = 1 - \frac{\omega_p^2}{\omega^2 + i\omega/\tau} \qquad \text{with} \quad \frac{1}{\tau} \ll \omega_p$$

and ω_p the plasmon frequency

then

$$\mathrm{Im}\,\frac{-1}{\varepsilon(\omega)+1} = \frac{\pi\hbar\omega_{sp}}{4}\,\delta(\hbar\omega - \hbar\omega_{sp})$$

where $\omega_{sp} = \frac{1}{\sqrt{2}}\,\omega_p$ is the

surface plasmon frequency. Then we learn that surface plasmons and all the so-called surface excitation are excited while the electron is still outside the material. Both plasmons excited while the electron is inside!

Thin Bulk/surface Plasmons

We now use the boundary condition

$$\underline{\mathcal{E}}_{i\parallel} = \underline{\mathcal{E}}_{ext\parallel} \qquad D_{i\perp} = D_{ext\perp}$$

to split the term under the integral using

$$\underline{\mathcal{E}}_i \cdot \underline{\dot{D}}_i = \varepsilon_s\, \mathcal{E}_{ext\parallel}\dot{\mathcal{E}}_{ext\parallel} + \frac{1}{\varepsilon_s}\, D_{ext\perp}\dot{D}_{ext\perp}$$

where ε_s is the dielectric constant of the layer. The losses of the layer are then

$$W = d\,8\pi^2 \int \omega\, d\omega\, dq_\parallel \left\{ \frac{\mathrm{Im}\,\varepsilon_s}{(\varepsilon_b+1)^2} \left|\mathcal{E}_{ext\parallel}(\omega, \underline{q}_\parallel)\right|^2 - \frac{\varepsilon_b^2}{(\varepsilon_b+1)^2}\,\mathrm{Im}\,\frac{1}{\varepsilon_s}\left|\mathcal{E}_{ext\perp}(\omega, \underline{q}_\parallel)\right.\right.$$

Suppose one has a dilute layer of molecules on a metal surface only the second term survives and we may replace

$$d \cdot \mathrm{Im}\,\frac{1}{\varepsilon_s} = 4\pi\,\mathrm{Im}\,\alpha(\omega) \cdot n_s$$

where $\alpha(\omega)$ is the polarizability of the molecules and n_s the surface density.

We proceede to calculate the Fourier-components $\mathcal{E}(\omega, q_\parallel)$ One uses

$$\frac{1}{r} = \frac{1}{2\pi}\int d\underline{q}_\parallel\, \frac{1}{q_\parallel}\, e^{-q_\parallel|z|}\, e^{-i\underline{q}_\parallel \cdot \underline{r}_\parallel}$$

$$-\nabla\frac{1}{r} = \frac{1}{2\pi}\int d\underline{q}_\parallel\, (i\underline{e}_\parallel, 1)\, e^{-q_\parallel|z|}\, e^{-i\underline{q}_\parallel \cdot \underline{r}_\parallel}$$

Dielectric losses of a thin layer on a substrate

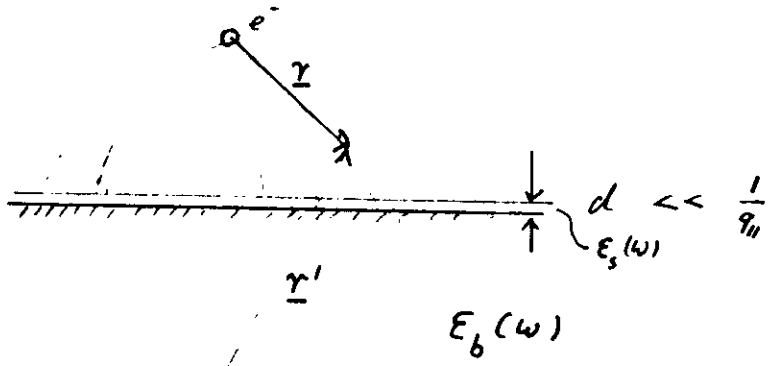

The potential outside the material is when $|d \cdot \varepsilon_s| \ll \varepsilon_b$

$$\varphi_a = e\left(\frac{1}{r} + \frac{1-\varepsilon_b}{1+\varepsilon_b}\frac{1}{r'}\right)$$

We calculate the vertical electric displacement $D_\perp$ and the parallel electric field $\mathcal{E}_\parallel$ at the surface

$$D_\perp\Big|_{z=0} = \frac{2\varepsilon_b}{1+\varepsilon_b} - \nabla_z \frac{e}{r}\Big|_{z=0} \qquad \mathcal{E}_\parallel\Big|_{z=0} = \frac{2}{\varepsilon_b+1} - \nabla_\parallel \frac{e}{r}\Big|_{z=0}$$

Note: $\frac{\partial}{\partial z}\frac{1}{r}\Big|_{z=0} = -\frac{\partial}{\partial z}\frac{1}{r'}\Big|_{z=0}$ $\qquad \frac{\partial}{\partial x}\frac{1}{r}\Big|_{z=0} = +\frac{\partial}{\partial x}\frac{1}{r'}\Big|_{z=0}$

When an electron is reflected at the surface

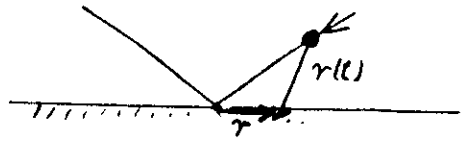

the vector $\underline{r}(t)$ is to be replaced by

$$r(t) = \underline{r} + \underline{v}_\parallel \underline{e}_\parallel t + v_\perp |t| \underline{e}_\perp$$

$$\mathcal{E}_{ext}(\underline{r}\,t) = -\nabla \frac{e}{|\underline{r} + \underline{v}_\parallel e_\parallel t + v_\perp |t| e_\perp|}$$

$$= \frac{1}{2\pi}\int d\underline{q}_\parallel (i e_\parallel, 1)\, e^{-i(\underline{q}_\parallel \underline{r}_\parallel + \underline{v}_\parallel t)}\, e^{-q_\parallel (z + v_\perp |t|)} \qquad z>0$$

Fourier expansion of the kernel

$$e^{-i\underline{q}_\parallel \cdot \underline{r}_\parallel t - q_\parallel v_\perp |t|} = \frac{1}{2\pi}\int d\omega\, e^{-i\omega t}\, \frac{2 q_\parallel v_\perp}{(\omega - \underline{q}_\parallel \underline{v}_\parallel)^2 + q_\parallel^2 v_\perp^2}$$

$$\Rightarrow \quad \mathcal{E}_{ext}(\omega, q_\parallel) = (i e_\parallel, 1)\frac{e}{(2\pi)^3}\, \frac{2 q_\parallel v_\perp}{(\omega - \underline{q}_\parallel \underline{v}_\parallel)^2 + q_\parallel^2 v_\perp^2}$$

From which we deduce for the loss probability

$$P(\omega, q_\parallel) = \frac{4 e^2 d n_s}{\pi^3}\, \frac{q_\parallel^2 v_\perp^2}{\left((\omega - \underline{q}_\parallel \underline{v}_\parallel)^2 + q_\parallel^2 v_\perp^2\right)^2}\, \mathrm{Im}\,\alpha_s(\omega)$$

4.2 Electron - ion core scattering inelastic LEED

Even for a well ordered surface one has plenty of intensity scattered in between the diffracted beam. This is the inelastic diffuse scattering due to the electron phonon interaction.

Remember: $I(\Pi)_{kk} = I^0_{kk}\, e^{-\sum_{q\nu} \frac{1}{2} \langle |(\underline{k}_i - \underline{k}_f)\cdot \underline{u}_{q\nu}(\omega)|^2 \rangle_T}$

The interaction between Electron and Solid is mediated via the Coulomb potential $V(\underline{r}_{el}, \{\underline{R}\})$ which depends parametrically on the coordinates of all nuclei.

The initial and final states of electrons and solid are described by:

$$|i\rangle = |k_i\rangle\, |n_i(Q_{\parallel 1}, j_1)\; n_i(Q_{\parallel 2}, j_2) \ldots\rangle$$

$$|f\rangle = |k_j\rangle\, |n_f(Q_{\parallel 1}, j_1)\; n_f(Q_{\parallel 2}, j_2) \ldots\rangle$$

where $Q_\parallel, j$ denotes the parallel momentum of the phonon and j the branch. Think of a slab of finite thickness.

The Matrix element for the transition from $|i\rangle$ to $|f\rangle$ is

$$M_{fi} = \langle f | T(E_i) | i\rangle \quad \text{with}$$

$T(E_i)$ the transfer operator

$$T(E) = V(\{\underline{R}\}) + V(\{\underline{R}\})\, G(E)\, T(E)$$

$G(E)$ is the free electron propagator

$$G(E) = \frac{1}{E - H_0 + i0} \qquad H_0 = \frac{p^2}{2m}$$

$T(E)$ depends also parametrically on the positions of the ion cores $\{\underline{R}\}$. The Matrix element may therefore be expanded around the average atom positions and thus also the scattering amplitude which is proportional to the Matrix element

$$f(\vec{k}_i, \vec{k}_f, \{\underline{R}\}) \sim M_{fi}$$

$$f(\vec{k}_i, \vec{k}_f, \{\underline{R}\}) = f(\underline{k}_i, \underline{k}_f, \{\underline{R}^0\}) + \sum_{\vec{l}_\parallel l_z\, K i} \left(\frac{\partial f}{\partial R_i(\vec{l}_\parallel, l_z K)}\right)_0 u_i(l_\parallel, l_z, K)$$

↑

LEED one-phonon scattering process

One has a kind of Bloch-Theorem for the derivatives

$$\frac{\partial f}{\partial R_i(\vec{l}_\parallel, l_z K)} = \frac{\partial f}{\partial R_i(0, l_z K)}\, e^{i \vec{R}^0(\vec{l}_\parallel, l_z K)\cdot \Delta \vec{K}_\parallel}$$

Kinematical approximation for a simple cubic lattice

$$f = f_0 \sum_{l_\parallel l_z} e^{i R(\vec{l}_\parallel, l_z)\cdot \Delta \vec{K}}$$

$$\left.\frac{\partial f}{\partial R_i(0 l_z)}\right|_0 = f_0\, i \Delta \vec{K}_i\, e^{i \Delta \vec{K}\cdot R^0(0, l_z)}$$

One has a product $u \cdot \Delta K$ appearing in the cross section

When the crystal has a mirror plane the modes divide into even and odd modes. Odd modes are polarized perpendicular to the plane when the plane runs through an atom

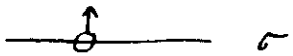

When ΔK is aligned with σ the cross section vanishes

selection rule

3 view graphs repeating the table

graph : cross section dynamical vs. kinematical
graph : surface modes vs. energy
graph : example agreement between theory and experiment

..1 A short excursion into elastic diffuse scattering

view graph : Fe overlayers on Cu(100)
ordered epitaxial growth up to five monolayers
view graph disordered oxygen on Ni(100)
view graph diffuse intensity as a function of concentration

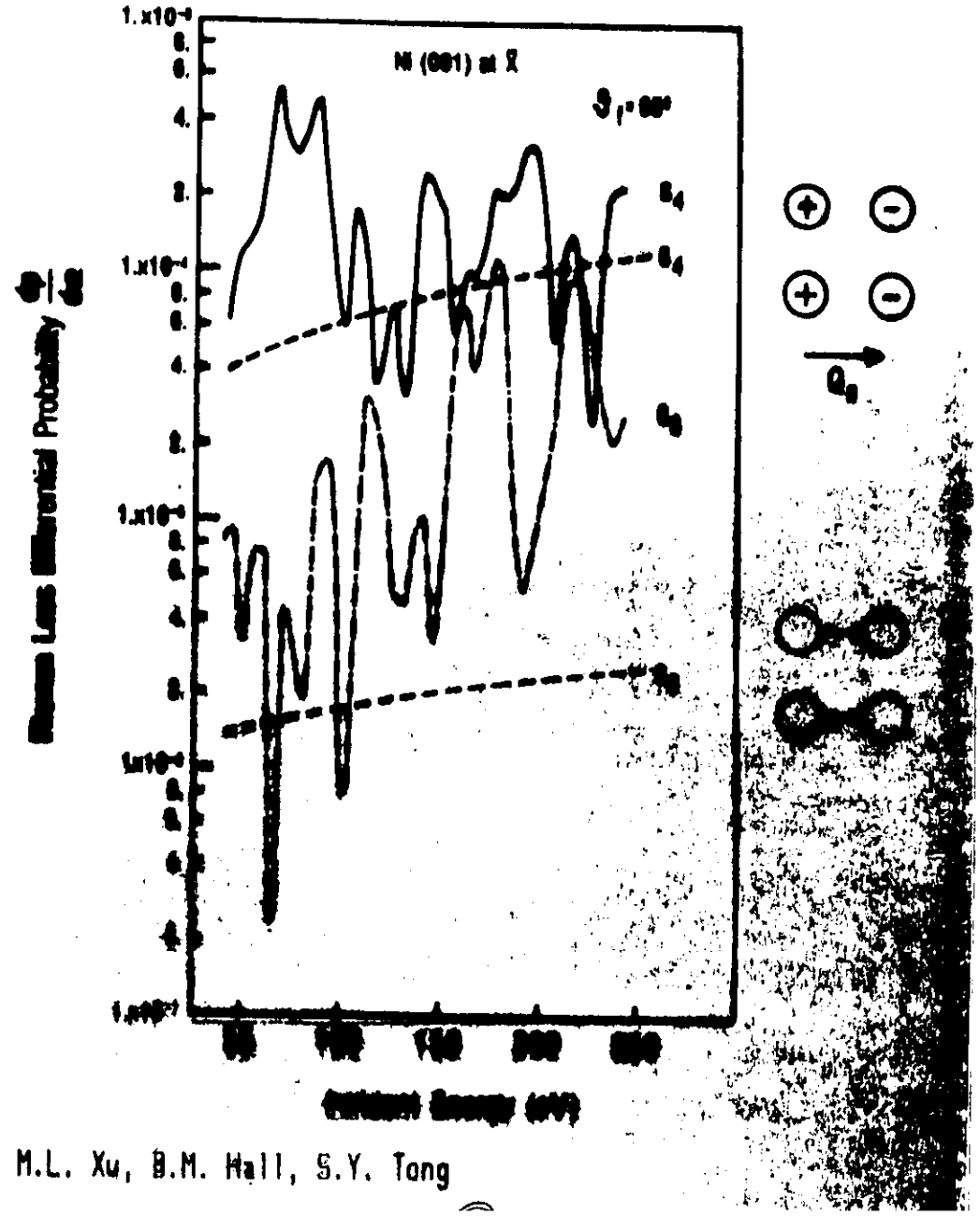

M.L. Xu, B.M. Hall, S.Y. Tong

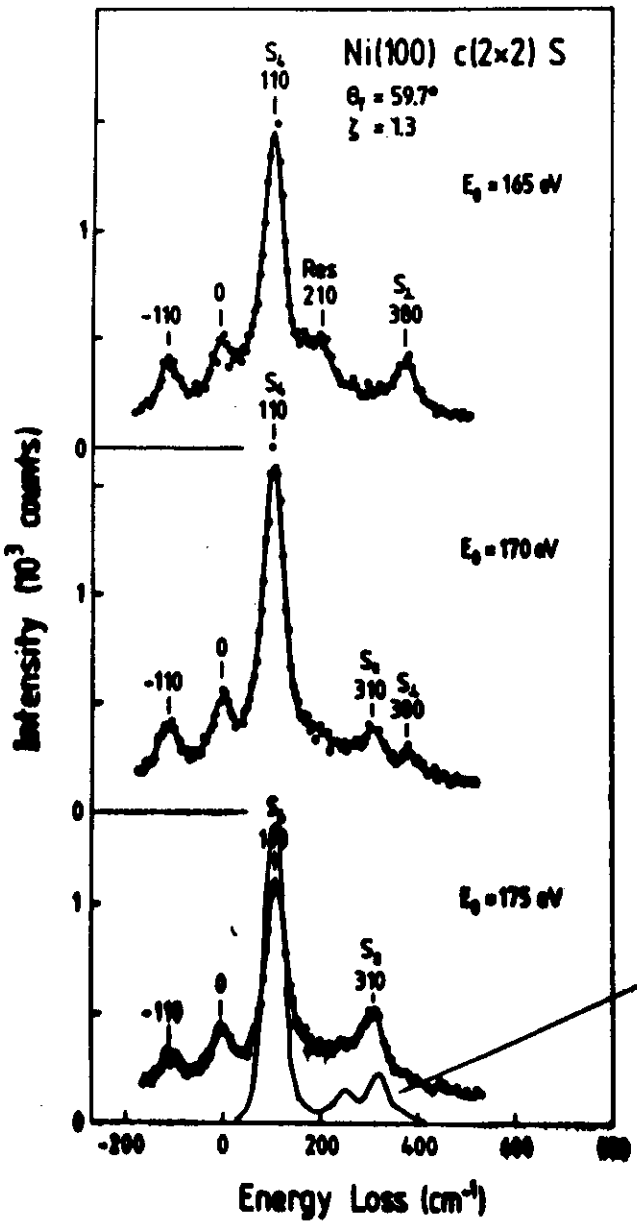

calc. Intensity

S.Y. Tong et al.

B. Hall

UCI

Dept. Physics

4.3 resonance scattering

Electronic structure of diatomic molecules

	orbital	no. electrons	bonding character
e.g. Oxygen	$\sigma_{g\uparrow\downarrow}(2s)$	2	bonding
	$\sigma_{u\uparrow\uparrow}(2s)$	2	anti
	$\sigma_{g\uparrow\downarrow}(2p)$	2	bonding
	$\pi_{u\uparrow\uparrow}(2p)$	4	bonding
	$\pi^*_{g\uparrow\downarrow}(2p)$	2	antibonding

The formal bond order is: $(2+2+4-2-2)/2 = 2$

The π^*_g orbital has room for two more electrons, which makes a resonance slightly above the ionization level

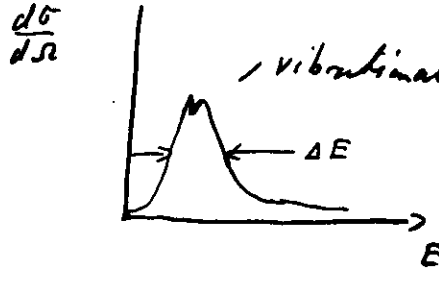

$\tau = \frac{\hbar}{\Delta E}$ life in π^* orbit

Characteristics of resonance scattering

1) Strong elastic and inelastic scattering at a particular E_{kin} (not $\vec{k}_i$).
2) High directionality of emitted electron

Possibility of measuring the orientation of molecules on surfaces.

View graph Fig 1 and 2 Palmer et al. PRL 60 329(1988)

Selection rule for shape resonance: The exiting electron in a shape resonance give rise to a force pulse, the symmetry of the force field is given by the symmetry of $|\Psi|^2$ which totally symmetric, when Ψ belongs to a non degenerate representation

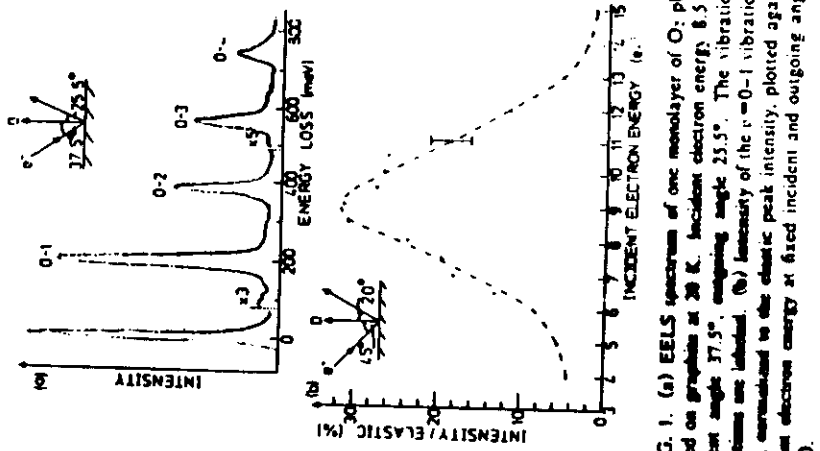

FIG. 1. (a) EELS spectrum of one monolayer of O_2 physisorbed on graphite at 20 K. Incident electron energy 8.5 eV, incident angle 37.5°, outgoing angle 25.5°. The vibrational transitions are labeled. (b) Intensity of the $v=0-1$ vibrational mode, normalized to the elastic peak intensity, plotted against incident electron energy at fixed incident and outgoing angles (inset).

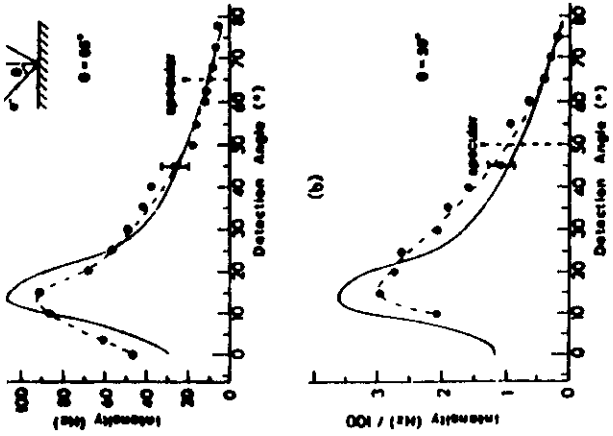

FIG. 2. Angular profile of electrons inelastically scattered after excitation of the $v=0-1$ transition in one monolayer of O_2 on graphite for two different angles of incidence, (a) 65° and (b) 50°. Temperature 18 K in (a) and 19 K in (b). The incident electron energy is 8.5 eV in both cases. The detection angle is labeled with respect to the normal to the crystal. The dashed lines are guides for the eye through the experimental points. The solid curves are the profiles calculated for electron emission from the $^3\Pi_u$ resonance of an O_2 molecule in the Ω phase with the molecular axis oriented at 25° from the normal to the surface. The intensity of each of the calculated profiles has been normalized by our equating the area under it with that under the corresponding experimental profile.

TABLE 3-4

Vibrational Frequencies of Some Common Bonds[a]

Group	Bond-stretching vibration, cm⁻¹	Group	Bond-stretching vibration, cm⁻¹	Group	Bond-bending vibration, cm⁻¹
≡C-H	3300	-C≡C-	2050	≡C-H	700
=C-H	3050	>C=C<	1650	=C(H)-H	1100
-C-H	2960	-C-C-	990	-C(H)(H)-H	1000
-O-H	3600	>C=O	1100	-O(H)-H	1400
-S-H	2570	>C=S	800	-S(H)-H	1400
-N-H	3400	>C=N-	1640	-N(H)-H	1600
>C=O	1700	>C-I	500		
-C≡N	2100				

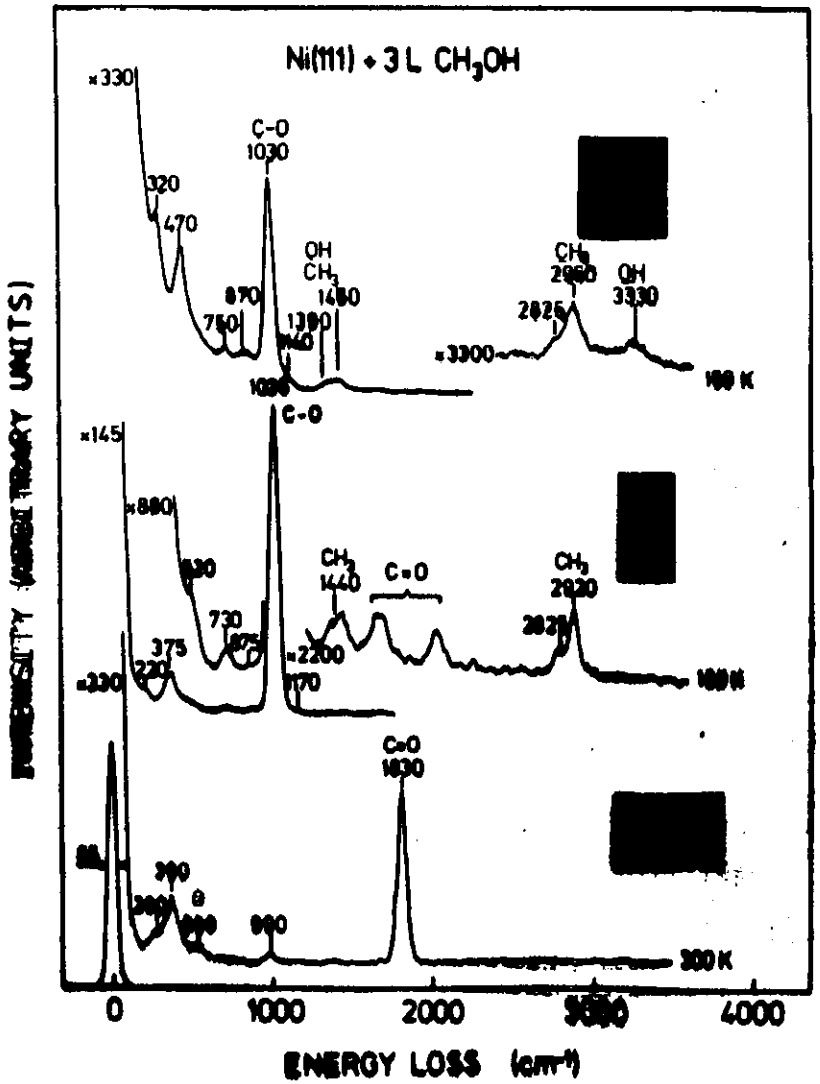

Characteristics of Dipole Losses

1. Dipole losses are confined to a narrow angular cone around the specular (diffracted) beam(s)

2. Differential cross section is high for CO, NO, O ...

3. One observes only losses of vibrations which belong to the same representation as z (ground state to first exited state)

4. Losses of a semi-infinite bulk are decribed by bulk optical constants

Examples of Dipole Active Modes

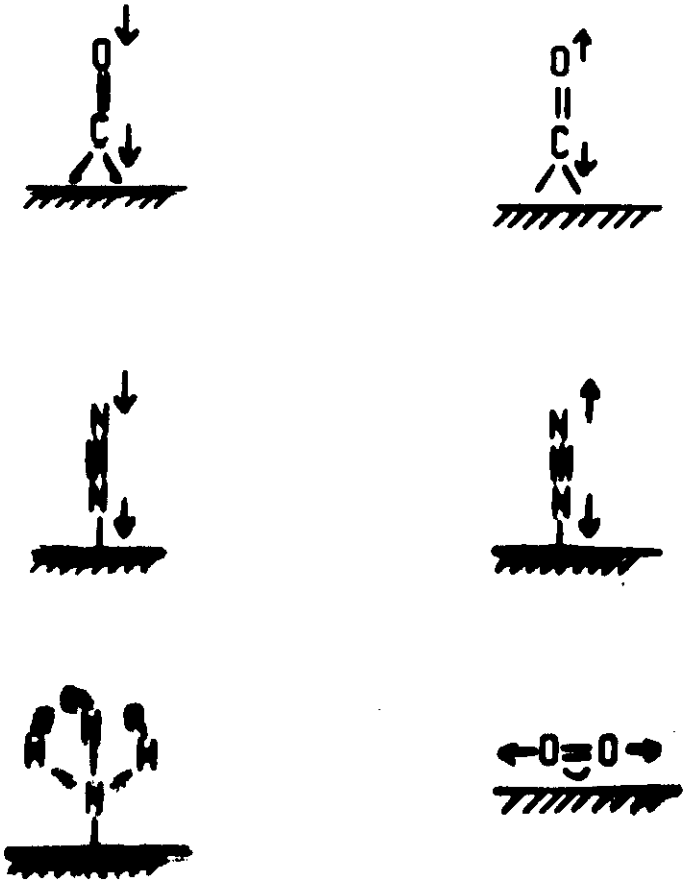

All modes of the total symmetric representation of the surface point group are dipole ective.

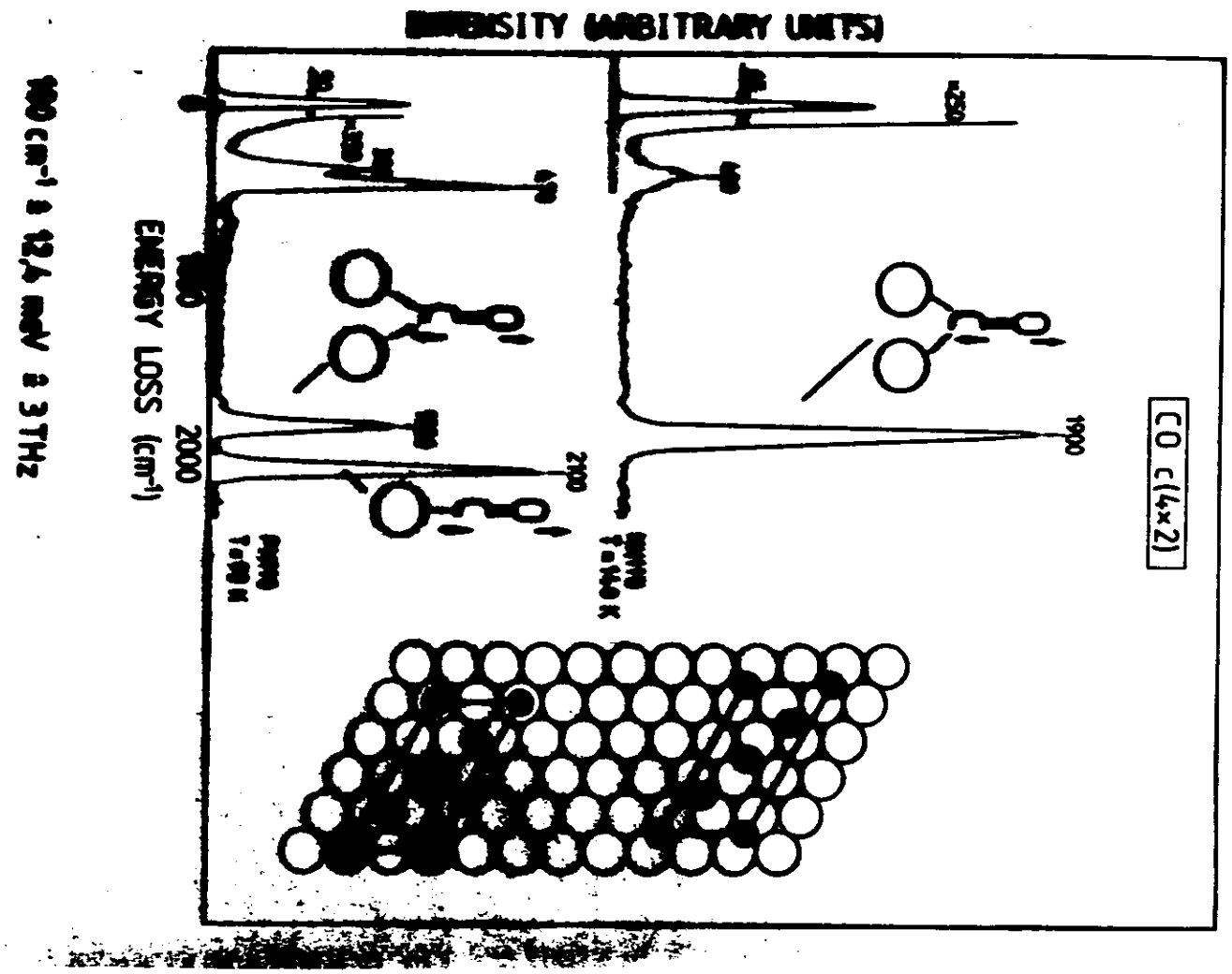
INTENSITY (ARBITRARY UNITS)
ENERGY LOSS (cm⁻¹)
2000
CO c(4×2)

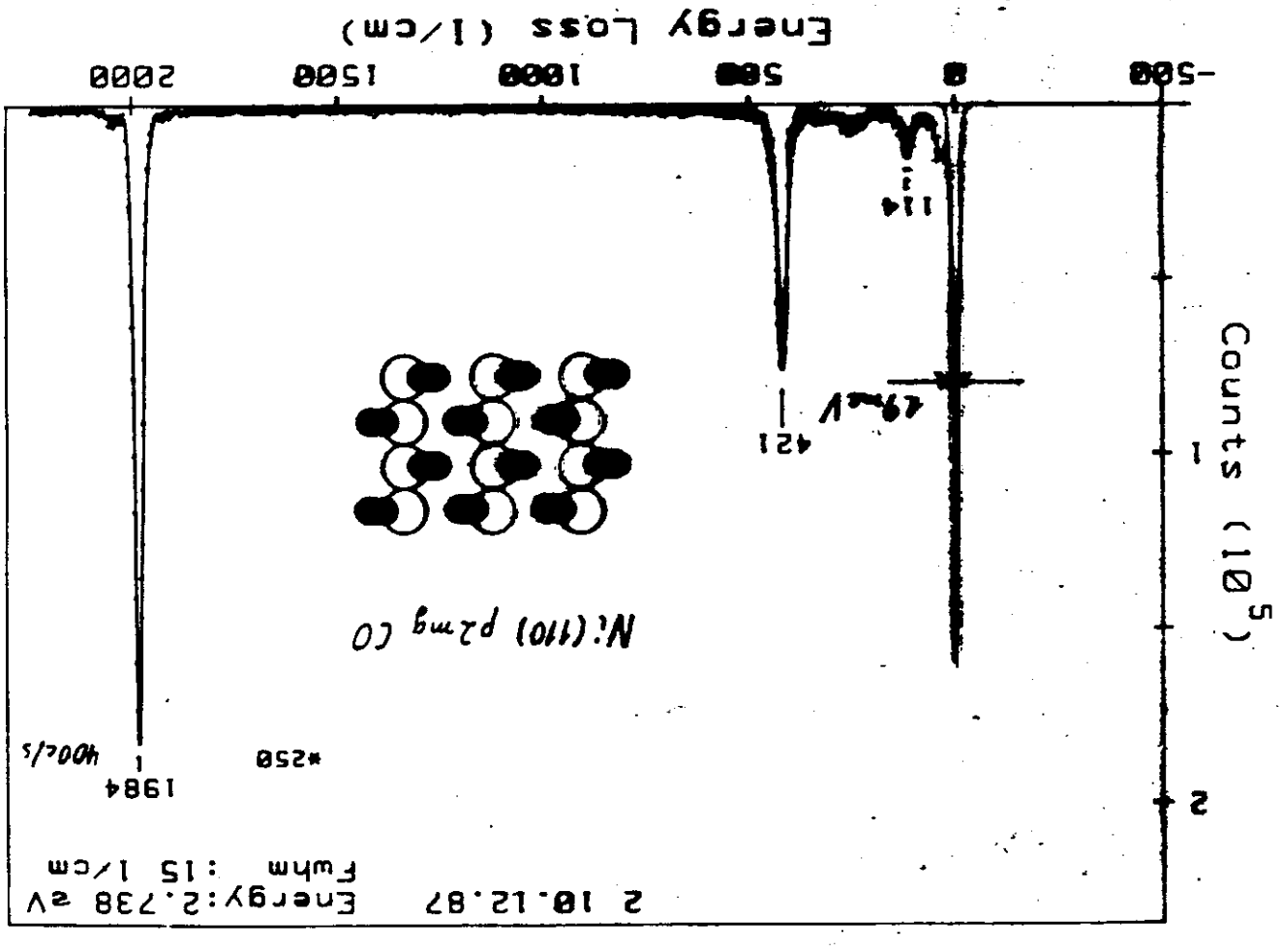
Energy Loss (1/cm)
2000
1500
1000
500
0
-500
Counts (10⁵)
2
1
421
114
Ni(110) p2mg CO
Energy:2.738 eV
Fwhm :15 1/cm
2 10.12.87
1984
*250

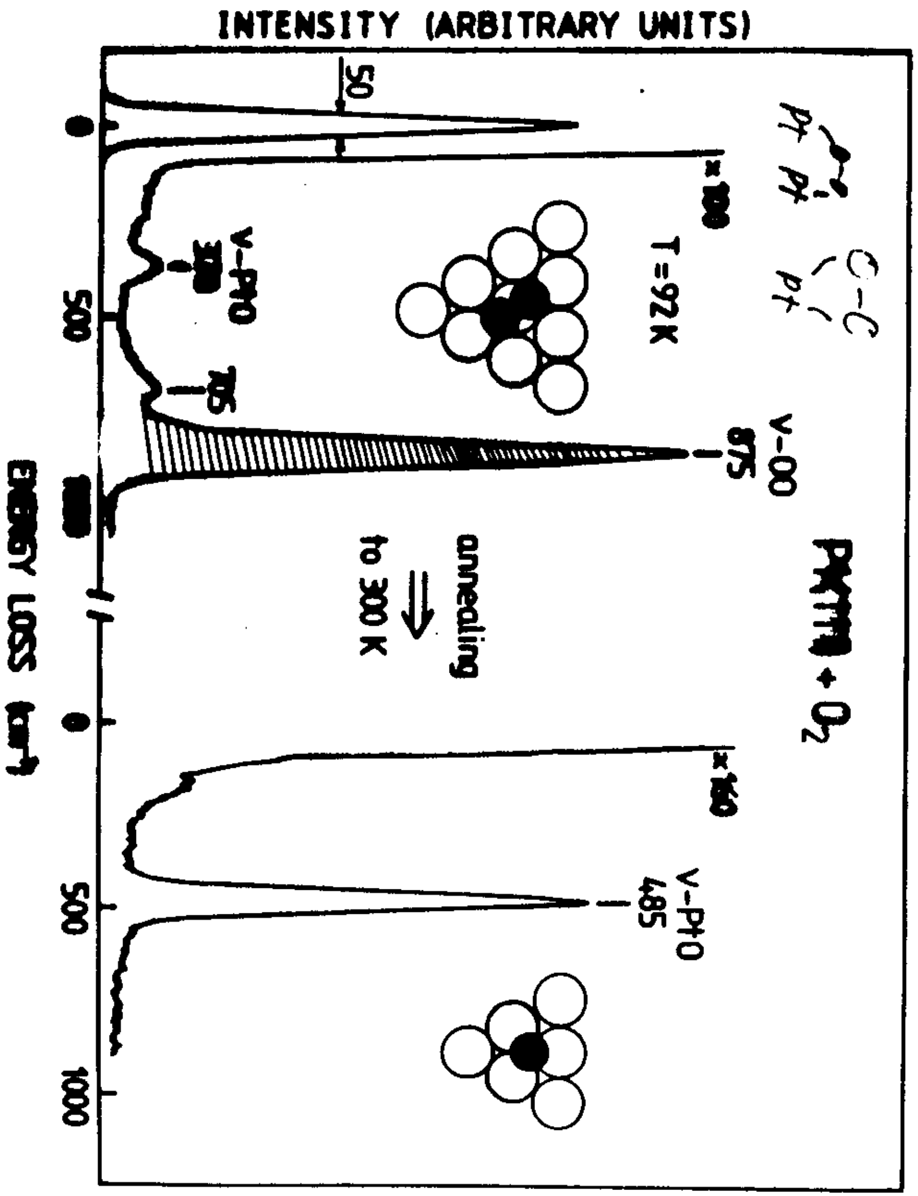

INTENSITY (ARBITRARY UNITS)
ENERGY LOSS (cm⁻¹)
Pt(111) + O2
T = 92 K
v-OO
875
v-PtO
485
annealing
to 300 K
x 100
x 160

(40)

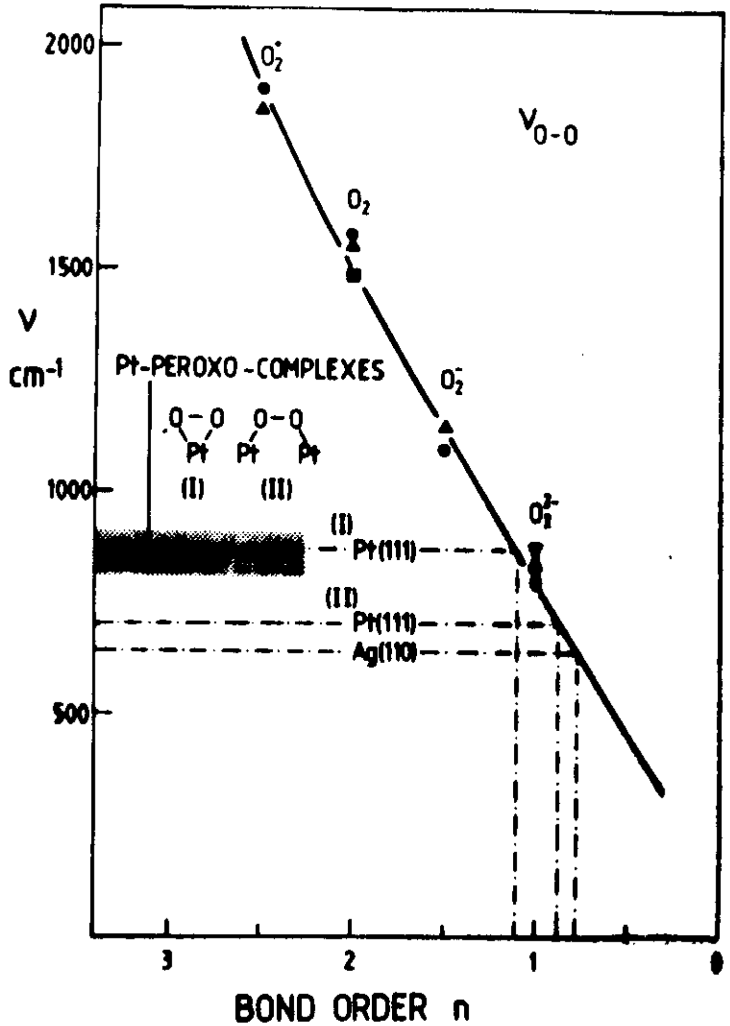

V
cm⁻¹
2000
1500
1000
500
V0-0
Pt-PEROXO-COMPLEXES
(I)
(II)
Pt(111)
Ag(110)
BOND ORDER n
3
2
1
0

(41)

What are Surface Phonons?

Take e.g. an adsorbed atom

dense, disordered layer

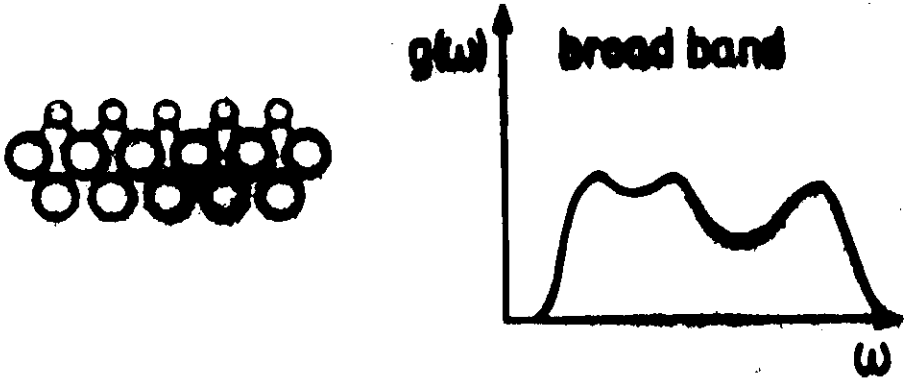

For ordered overlayers the eigensolutions are two-dimensional waves and for each wave with wavevector $\underline{q}_{\parallel}$ one has three frequencies

General form of the eigensolution

$$\underline{e}(l_z, \underline{q}_{\parallel}, \omega) = \underline{e}(l_z, \underline{q}_{\parallel})\, e^{-i(\omega t - \underline{q}_{\parallel} \cdot \underline{r}_{\parallel})}$$

Phonon dispersion of adsorbate modes (scematic)

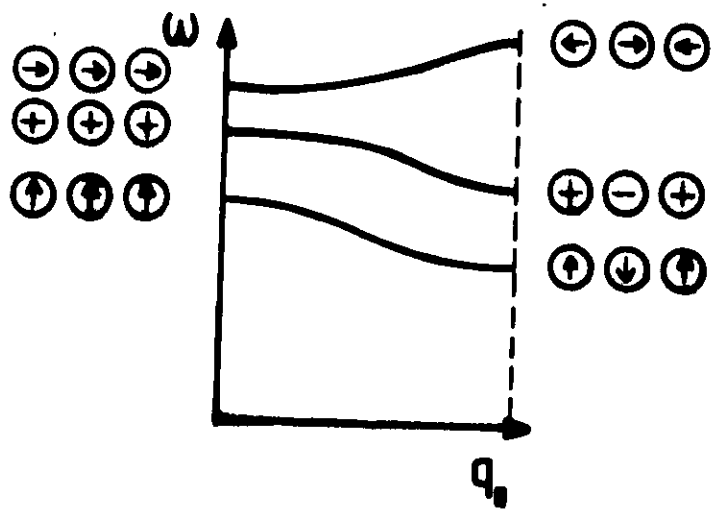

In scattering experiments on has

$E' - E = \pm \hbar\omega$ energy conservation

$\underline{k}'_{\parallel} - \underline{k}_{\parallel} = \underline{q}_{\parallel} + \underline{G}_{\parallel}$ wave vector conservation

The dispersion is a measure of the lateral vibrational coupling

A case of very strong lateral coupling is the coupling between the surface atoms of the substrate

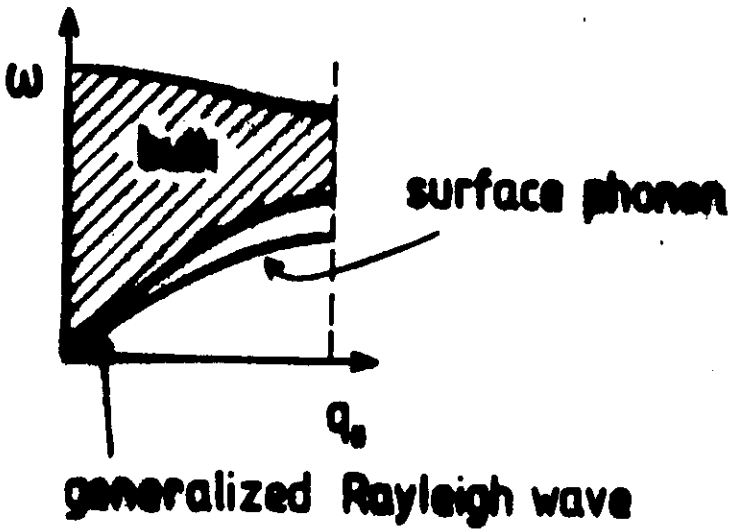

Displacement Vectors in a Rayleigh-Wave

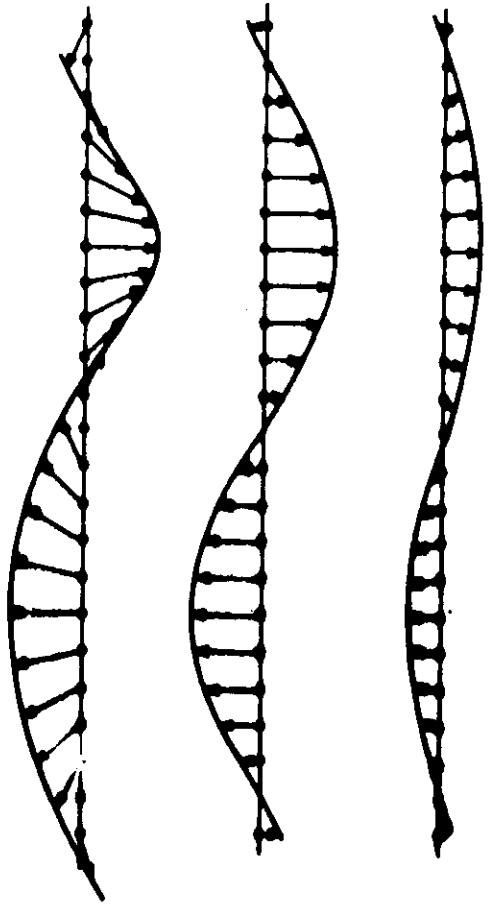

Lord Rayleigh, Proc. London Math. Soc. 17, 4 (1887)

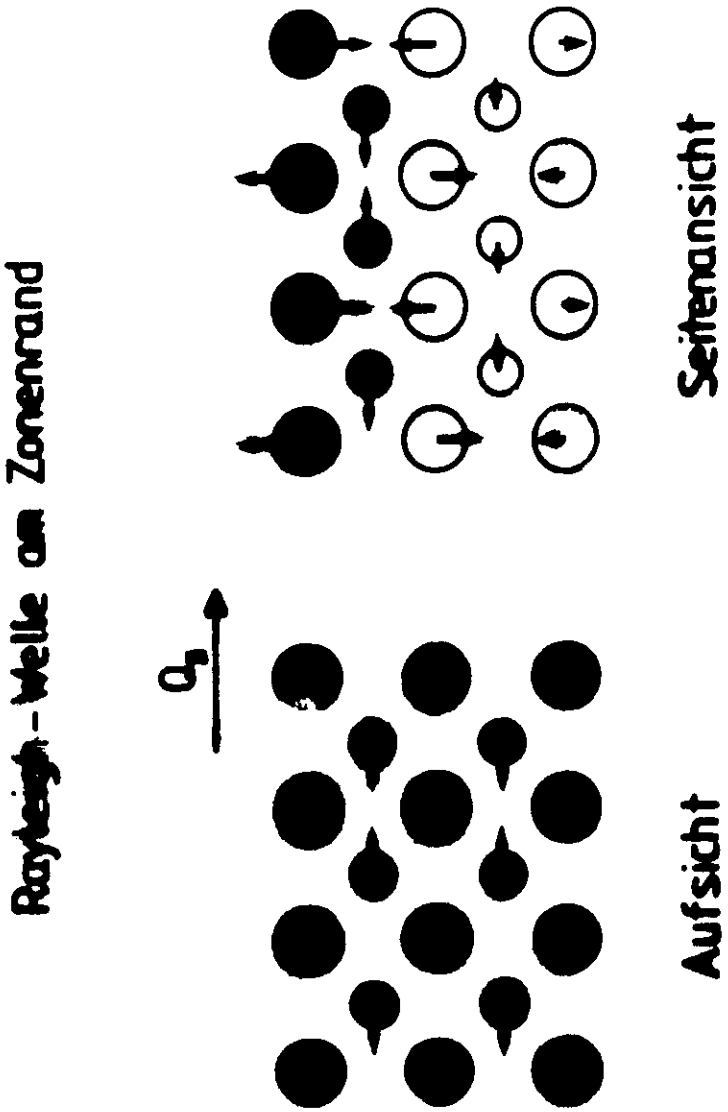

A very unique example of a substrate surface phonon!

(100) surface of an fcc or bcc lattice

$$m\omega^2 = 4k_{12}\cos^2\theta$$

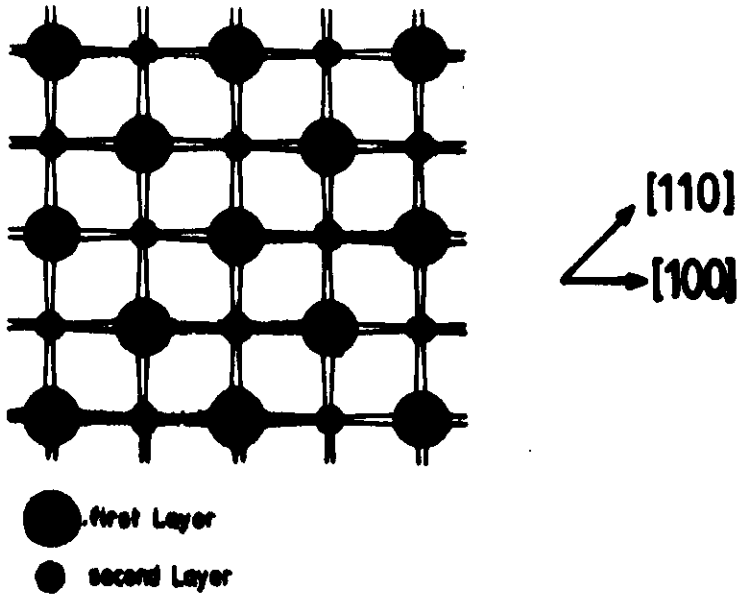

The second layer does not move!
All forces on the second layer atoms cancel!

$\Rightarrow$ this mode probes directly the bond between the first and second layer!

Surface Lattice Dynamics

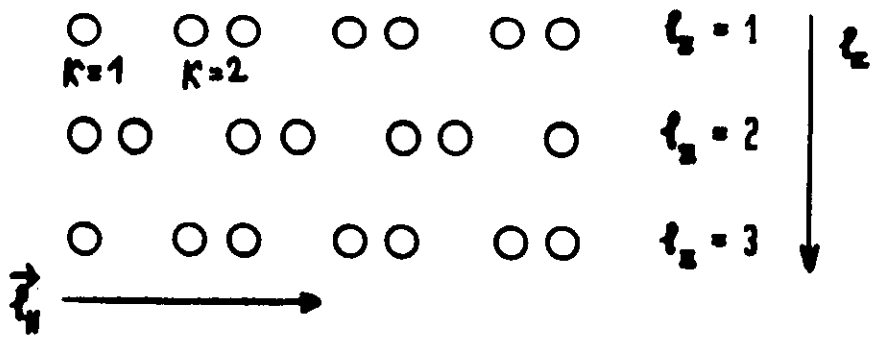

Equilibrium position: $\vec{R}_0(\vec{\ell}_\parallel, \ell_2, \kappa)$

Displacements: $u_\alpha(\vec{\ell}_\parallel, \ell_2, \kappa)$

Equation of motion

$$M(\ell_2\kappa)\,\ddot{u}_\alpha(\vec{\ell}_\parallel\ell_2\kappa) + \sum_{\beta\vec{\ell}'_\parallel\ell'_2\kappa'} \phi_{\alpha\beta}(\vec{\ell}_\parallel\ell_2\kappa;\vec{\ell}'_\parallel\ell'_2\kappa')\,u_\beta(\vec{\ell}'_\parallel\ell'_2\kappa') = 0$$

with mass reduced coordinates

$$u_\alpha(\vec{\ell}_\parallel\ell_2\kappa) = [M(\ell_2\kappa)]^{-\frac{1}{2}}\,\xi_\alpha(\vec{\ell}_\parallel\ell_2\kappa)\,e^{-i\omega t}$$

$$\ddot{\xi}(\vec{\ell}_\parallel\ell_2\kappa) + \sum_{\beta\vec{\ell}'_\parallel\ell'_2\kappa'} \frac{\phi_{\alpha\beta}(\vec{\ell}_\parallel\ell_2\kappa;\vec{\ell}'_\parallel\ell'_2\kappa')}{[M(\ell_2\kappa)\,M(\ell'_2\kappa')]^{\frac{1}{2}}}\,\xi_\alpha(\vec{\ell}'_\parallel\ell'_2\kappa') = 0$$

For periodic surfaces the $\phi_{\alpha\beta}$ depend only on the difference $\vec{\ell}_\parallel - \vec{\ell}'_\parallel$. The secular equation admits solutions of the form

$$\xi_\alpha(\vec{\ell}_\parallel\ell_2\kappa) = \exp\left[i\,\vec{Q}_\parallel\cdot\vec{R}_0(\vec{\ell}_\parallel\ell_2\kappa)\right] e_\alpha(\vec{Q}_\parallel;\ell_2\kappa)$$

The secular equation then assumes the form

$$\omega^2 e_\alpha(\vec{Q}_\parallel;\ell_2\kappa) - \sum_{\beta\ell'_2\kappa'} d_{\alpha\beta}(\vec{Q}_\parallel;\ell_2\kappa;\ell'_2\kappa')\,e_\beta(\vec{Q}_\parallel;\ell'_2\kappa') = 0$$

with

$$d_{\alpha\beta}(\vec{Q}_\parallel;\ell_2\kappa;\ell'_2\kappa') = \sum_{\vec{\ell}_\parallel} \frac{\phi_{\alpha\beta}(\vec{\ell}_\parallel\ell_2\kappa;\vec{\ell}'_\parallel\ell'_2\kappa')}{[M(\ell_2\kappa)\,M(\ell'_2\kappa')]^{\frac{1}{2}}}\,e^{\,i\,\vec{Q}_\parallel\cdot[\vec{R}_0(\vec{\ell}_\parallel\ell_2\kappa) - \vec{R}_0(\vec{\ell}'_\parallel\ell'_2\kappa')]}$$

In this notation $d_{\alpha\beta}$ is hermitean with respect to $\ell_2\kappa$, $\ell'_2\kappa'$

The secular equation may be solved for a finite number of layers: "slab method"

Green's Function Method

One defines the (Fourier transformed) Green's function

$$U_{\alpha\beta}(\ell_1\kappa,\ell_2\kappa';\vec{Q}_\parallel\omega) = \sum_s \frac{e_\alpha^{(s)}(\vec{Q}_\parallel;\ell_1\kappa)\, e_\beta^{(s)*}(\vec{Q}_\parallel;\ell_2\kappa')}{\omega^2 - \omega_s^2(\vec{Q}_\parallel)}$$

This function satisfies

$$\omega^2 U_{\alpha\beta}(\ell_1\kappa,\ell_2\kappa';\vec{Q}_\parallel\omega)$$

$$-\sum_{\ell''\kappa''}\sum_\gamma d_{\alpha\gamma}(\vec{Q}_\parallel;\ell_1\kappa,\ell''\kappa'')\, U_{\gamma\beta}(\ell''\kappa'';\ell_2\kappa';\vec{Q}_\parallel\omega) = \delta_{\alpha\beta}\,\delta_{\ell_1\ell_2}\,\delta_{\kappa\kappa'}$$

These equation are solved for the surface layers and the bulk by invoking an exponential ansatz. From U one calculates the "spectral densities"

Spectral Densities

$$S_{\alpha\beta}(\ell_1\kappa,\ell_2\kappa';\vec{Q}_\parallel\omega) \equiv \sum_s e_\alpha^{(s)}(\vec{Q}_\parallel;\ell_1\kappa)\, e_\beta^{(s)*}(\vec{Q}_\parallel;\ell_2\kappa')\,\delta(\omega-\omega_s(\vec{Q}_\parallel))$$

$$= \lim_{\varepsilon\to 0}\left\{i\,\frac{\omega}{\pi}\left[U_{\alpha\beta}(\ell_1\kappa,\ell_2\kappa';\vec{Q}_\parallel\omega+i\varepsilon) - U_{\alpha\beta}(\ell_1\kappa,\ell_2\kappa';\vec{Q}_\parallel\omega-i\varepsilon)\right]\right\}$$

One is mainly interested in the diagonal terms

$$\tilde{S}_\alpha(\ell_1\kappa;\vec{Q}_\parallel\omega) \equiv \sum_s |e_\alpha(\vec{Q}_\parallel;\ell_1\kappa)|^2\,\delta(\omega-\omega_s(\vec{Q}_\parallel))$$

This is the main physical quantity of interest For a semiinfinite crystal $\tilde{S}$ is a continuus function with δ-functions for the surface phonons. If $\tilde{S}$ is calculated with the slab method the δ-functions are replaced by Lorenzians.

Force Constants

The frequencies of surface phonons provide information on the force constants.

However: In order to extract this information one needs to make some assumptions about the type and range of the force field.

Different force fields may fit the data in a different manner. Physical intuition as well as guidance by total energy calculations is required. A useful strategy is to take a simple model which fits the bulk phonon dispersion and modify the force constants near the surface.

Surface Stress $\mathcal{T}$ and Surface Free Energy G_s in Creating a Surface of Area l^2

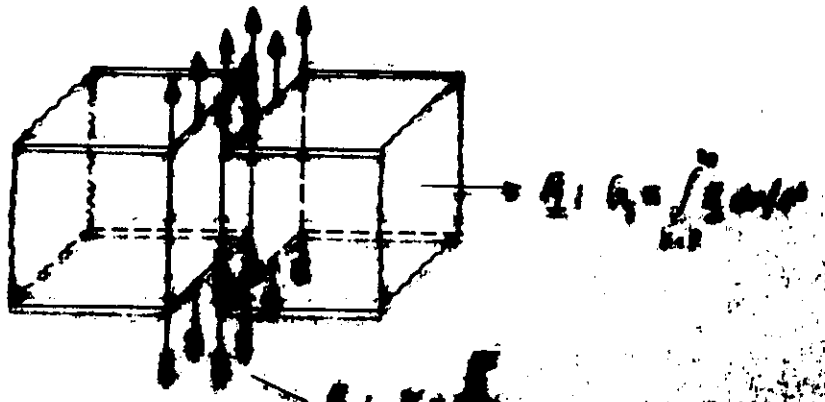

Surface stress and central force constant model

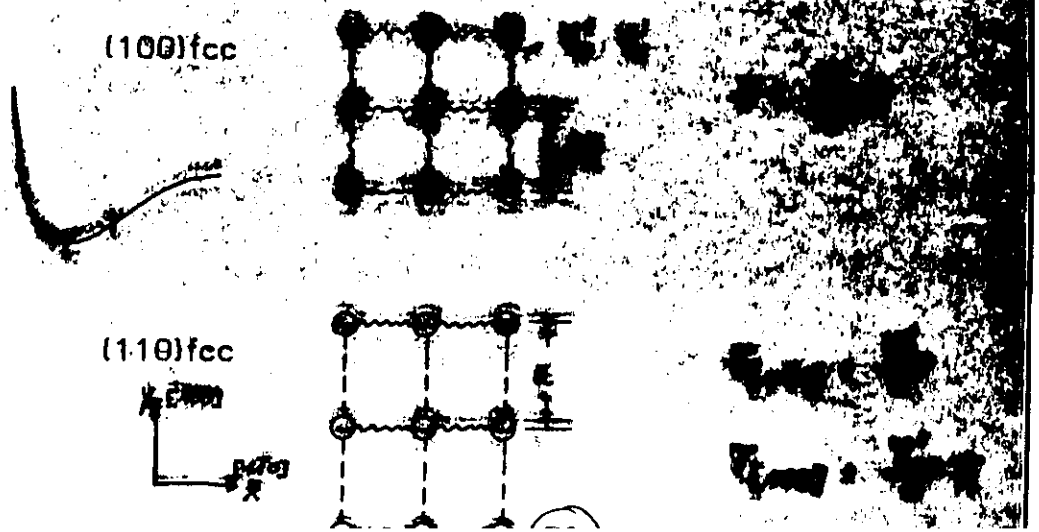

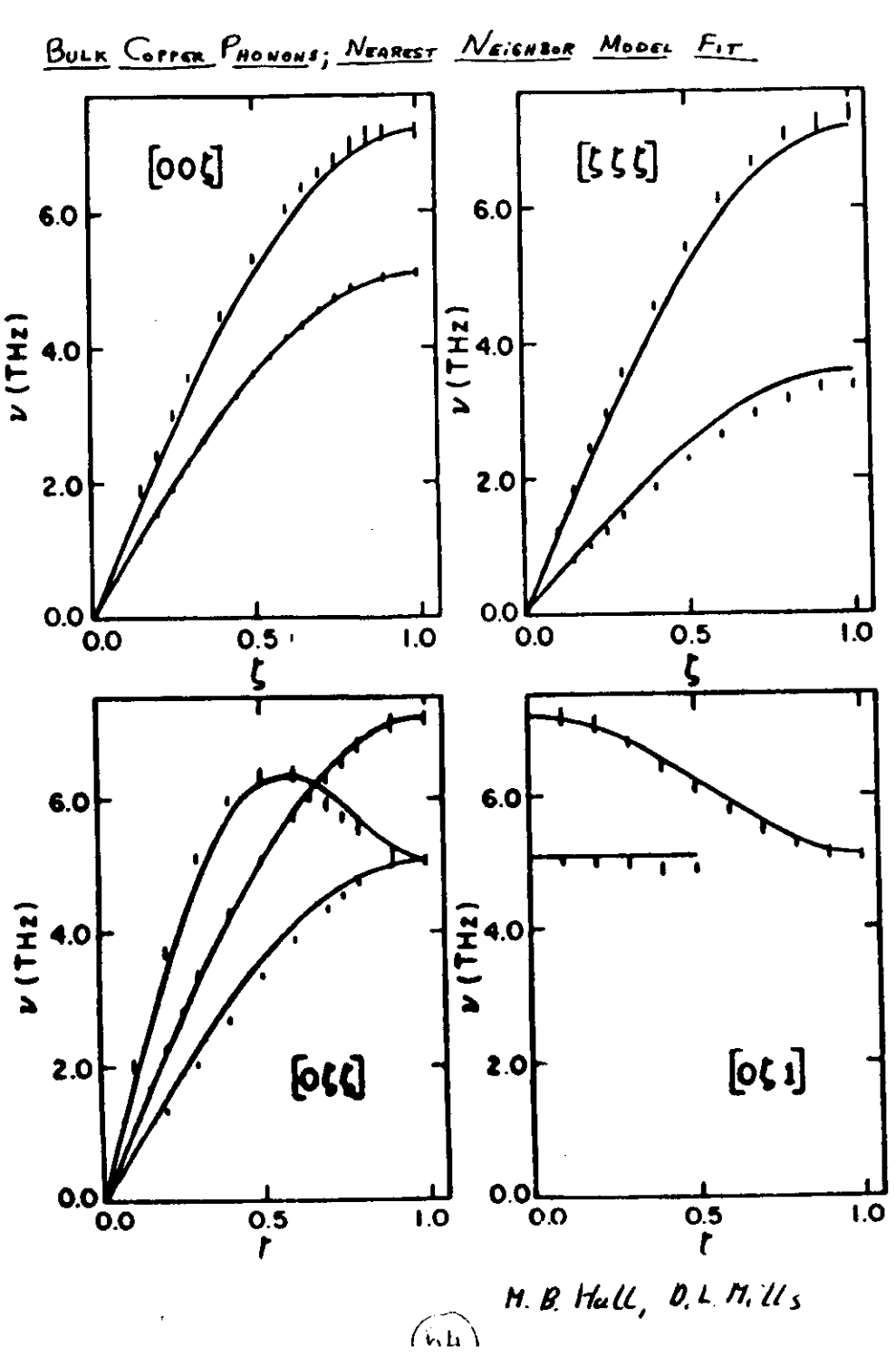

Stepwise Determination of the Surface Force Field

Nearest neighbor central force model(which fits the bulk), all surface force constants equal φ_b''

Step 1:The interlayer distances near the surface are contracted and expanded,respectively
$\Delta d_{12}/d_{12} = -9.6\%$, $\Delta d_{23}/d_{23} = +3.5\%$

We scale the interlayer force constants according to

$$\varphi_{ij}'' = \varphi_b'' \left(\frac{r_b}{r_{ij}} \right)^{\alpha}$$

α is taken such as to match the resonance mode at $\bar{\Gamma}$

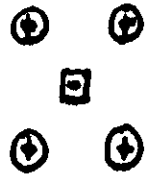

This mode is not at all affected by any intralayer force constant

Eigenvectors for Surface Modes on (110) f.c.c.

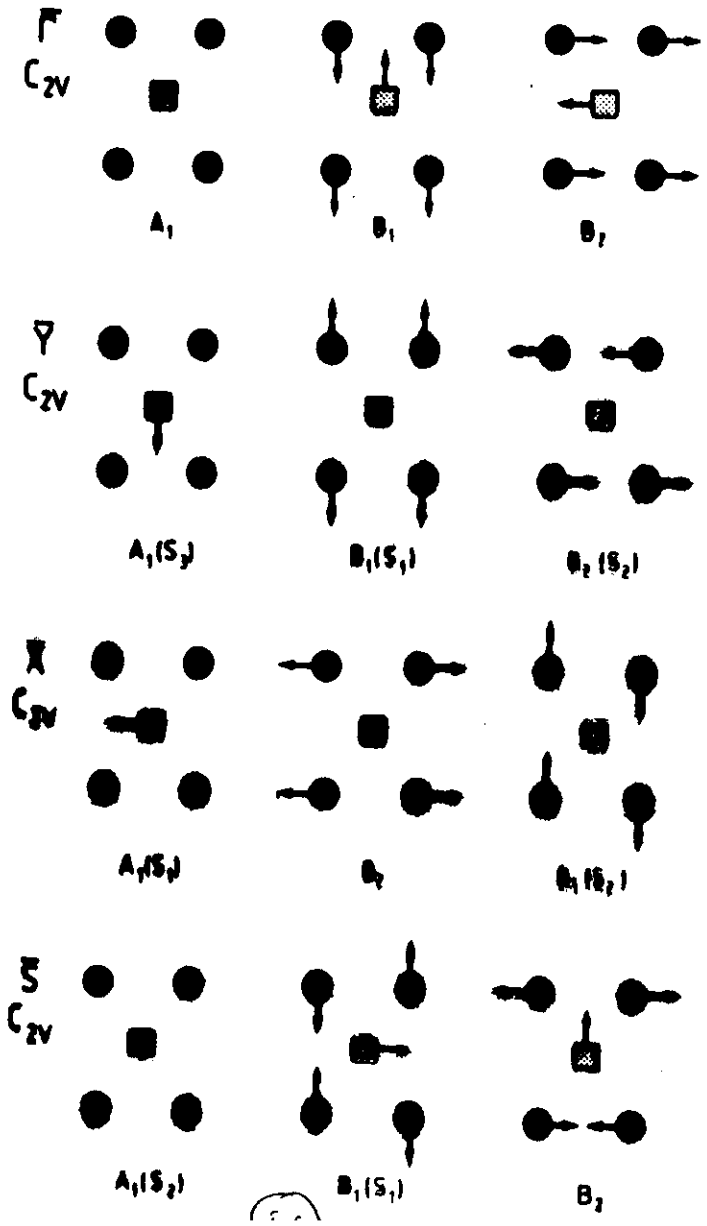

Surface Phonon Ni(110): Fitting Procedure

Surface mode		ω_{exp}	$\omega_{fit}(\Delta)$ fit parameter		ω_{fit}
$\omega(A_1,\bar{\Gamma})$		197	184	$\varphi''_{ij}=\varphi''_b(r_b/r_{ij})^6$	195
$\omega(A_1,\bar{X})$		137	127	$\varphi'_{110}=0.05a\cdot\varphi''_b$	137
$\omega(B_2,\bar{X})$	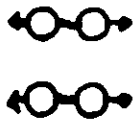	226	248	$\varphi''_{\parallel}=0.8\cdot\varphi''_b$	230
$\omega(A_2,\bar{Y})$		125	116	$\varphi'_{[001]}=0.08a\cdot\varphi''_b$	126
$\omega(B_2,\bar{Y})$		80	91	$\varphi''_{\parallel(4)}=-0.075\cdot\varphi''_b$	82

The Physics Behind the Fitting Procedure

1.)internal consistency: a.)once α is set the modes respond to the remaining parameters independently
b.) the force field fits also $\vec{S}$ direction and modes at other q,where the modes are of mixed polarisation

2.)the numbers appear to be reasonable considering the expected rearrangement of charge
⇒ pair potential curves

3.)the model accounts for the observed cross sections comparison theory—experiment

4.) reasonable values for the surface stress:

	our fit	Need's calculation for Al(110)
$\mathcal{T}_{110}$	$2.15 \cdot 10^3$ dynes/cm	$2.00 \cdot 10^3$ dynes/cm
$\mathcal{T}_{100}$	$4.20 \cdot 10^3$ dynes/cm	$1.85 \cdot 10^3$ dynes/cm

Charge Redistribution Near a Free Surface

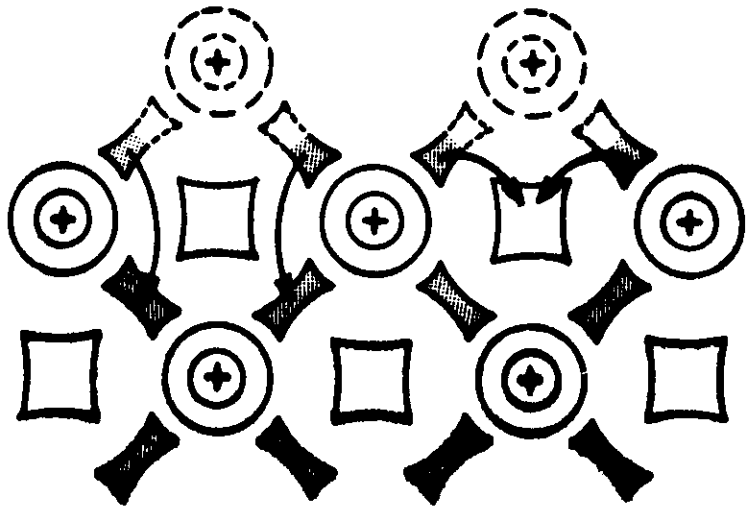

1. enhanced bond charge between first and second layer:
   ⟹ increased force constant,
   contraction

2. enhanced bond charge between surface atoms:
   ⟹ increased intralayer force constant,
   attractive surface stress

Adsorbate Induced Surface Stress and Reconstruction

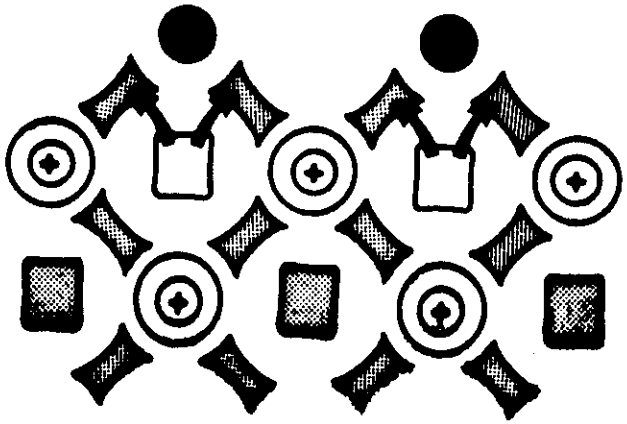

Application to O, N, C on Ni(100)

1. Adsorbate–substrate bonding removes charge from surface intralayer Ni–Ni bonds.

   ⇒ intralayer repulsive surface stress $\bar{\Gamma}'_{\parallel}$

2. Lattice dynamics show that frequency of Rayleigh wave at $\bar{X}$ is reduced (observed for oxygen)

3. As $\bar{\Gamma}'_{\parallel}$ increases the A_2–mode at $\bar{X}$ becomes soft.

4. The observed p4g structure for carbon and nitrogen correspond to a frozen A_2–phonon at $\bar{X}$

Epitaxial growth of metal–on–metal overlayers

Some unique properties:

1. Possibility of growing perfect crystals with low impurity level on the surface
2. Quantum size effects
3. Opportunity to produce metastable phases of material
4. Unusual electronic and mechanical properties
5. Microscopic understanding of conditions for epitaxial growth

We have studied structure and phonon dynamics of

Ag(111) on Ni(100)
Ag(111) on Cu(100)
fcc Fe(100) on Cu(100)
(fcc) Fe (100) on Ni(100)

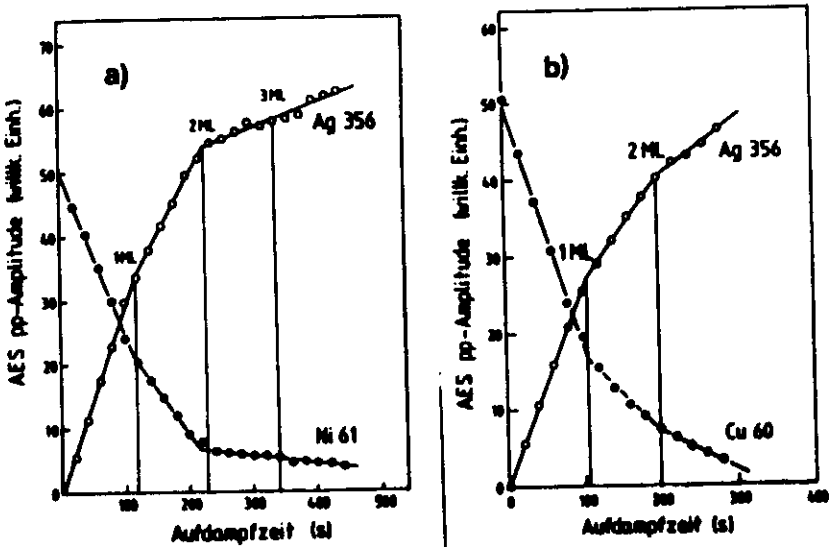

Abb. 6.1 Intensität der Ag 356-eV-Augerlinie und der Ni 61 eV-Augerlinie (a) bzw. Cu 60 eV-Augerlinie (b) als Funktion der Aufdampfzeit. Das stückweise lineare Verhalten der Funktionen in beiden Fällen ist charakteristisch für epitaktisches Lagenwachstum und liefert eine absolute Lagenkalibrierung.

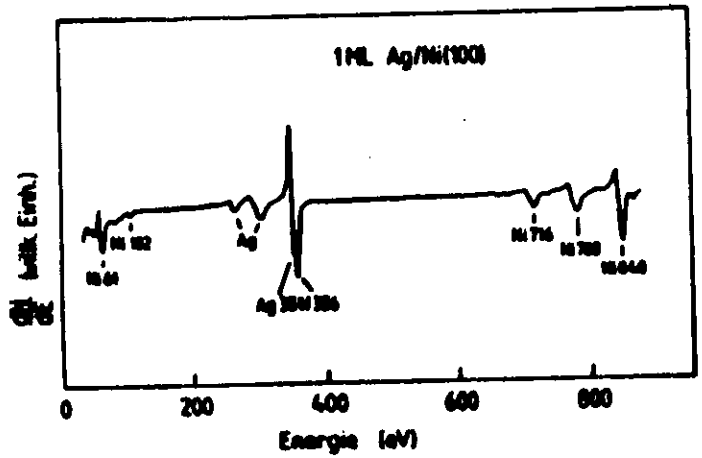

Abb. 6.2 Augerelektronenspektrum der Monolage Ag auf Ni(100).

(62)

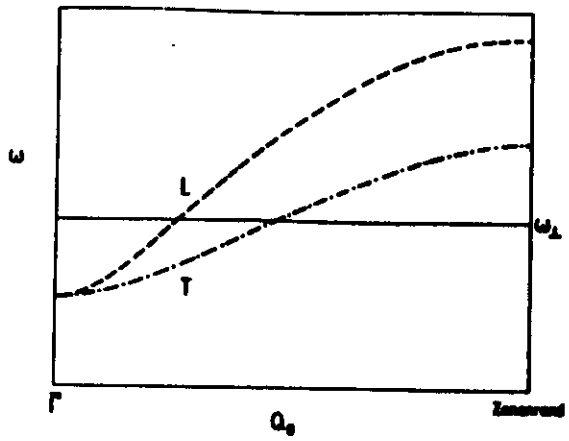

Abb. 6.14 Phononendispersion für eine geordnete Monolage von Adatomen auf einem starren Substrat. Die vertikale polarisierte Mode (durchgezogene Linie) ist immer dispersionslos, wenn die laterale Wechselwirkung der Adatome durch Zentralkraftkonstanten vermittelt wird.

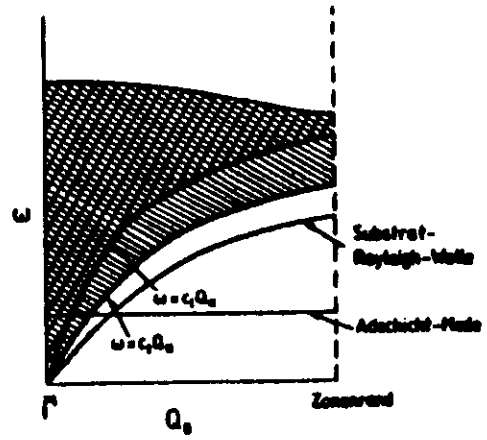

Abb. 6.15 Schematische Darstellung der Moden-Struktur eines Adschicht-Substrat-Systems. Neben der dispersionslosen Mode der vertikalen Schwingungen der Adatome sind die Substrat-Rayleigh-Welle sowie die Projektion der Substrat-Volumenphononen eingezeichnet.

Epitaxial Layers of fcc Iron on Cu(100)

Epitaxial growth up to 5 monolayers when substrate is held at 300 K. Interdiffusion at higher temperatures. Unusual magnetic properties: Magnetization parallel to the surface for 1 Monolayer, however perpendicular for 2–5 Monolayers!

W. Daum, C. Stuhlmann:

1. Monolayer grows as 5x1

2. 2 Monolayers display a reversible displacive phase transition between 2x1 at low temperatures and an ordered 1x1 at 300 K. A unique case in surface physics.

3. It is shown that the reconstruction is a direct consequence of the fact that the Fe–lattice is under lateral stress